Structure of ^{209}Bi deduced from the ^{208}Pb$(t,2n\gamma)$ reaction

K. H. Maier
Hahn-Meitner Institute, Berlin, Federal Republic of Germany and Florida State University, Tallahassee, Florida 32306

T. Nail, R. K. Sheline, and W. Stöffl
Florida State University, Tallahassee, Florida 32306

J. A. Becker, J. B. Carlson, R. G. Lanier, L. G. Mann, and G. L. Struble
Lawrence Livermore National Laboratory, Livermore, California 94550

J. A. Cizewski* and B. H. Erkkila
Los Alamos National Laboratory, Los Alamos, New Mexico 87545
(Received 29 July 1982)

States in ^{209}Bi were populated with the ^{208}Pb$(t,2n)$ reaction. Incident triton energies between 11 and 16 MeV were used. Gamma-ray excitation functions, angular distributions, and γ-γ-time coincidence spectra were measured. Approximately 50 newly-observed γ rays have been assigned to transitions in ^{209}Bi. Previously-unresolved doublets at $E_x=2600$, 3135, and 3154 keV have been identified. A new level at 3270 keV is reported, and the 3197-keV level is verified. ^{209}Bi level energies are reported with an accuracy of 600 eV or less. A level scheme for $E_x<4.14$ MeV is presented, including spin-parity assignments. A new $M1$ transition between the $\frac{5}{2}^+$ and $\frac{3}{2}^+$ members of the $\pi h_{9/2}\otimes 3^-$ septuplet is reported. The 19 levels belonging to the $\nu g_{9/2}p_{1/2}{}^{-1}$, $\pi h_{9/2}$ are identified.

NUCLEAR REACTIONS ^{208}Pb$(t,2n\gamma)^{209}$Bi, $E_t=11$–16 MeV. Measured E_γ, $I_\gamma(\theta)$, excitation functions, $\gamma\gamma t$ coinc. Deduced levels E, J^π, core-coupled multiplet structure.

I. INTRODUCTION

The nucleus ^{209}Bi consists of the doubly magic ^{208}Pb core and one valence proton. Due to this particularly simple structure it has played an essential role in the understanding of nuclear structure and reaction mechanisms. In this article we address the interplay between single-particle excitations and the coupling of the valence proton to the collective excitations of the ^{208}Pb core. The well-known septuplet of states arising from the coupling of the $h_{9/2}$ proton to the highly collective octupole vibration of the ^{208}Pb core at $E_x=2.62$ MeV is probably the best example of particle-vibration coupling. However, the states arising from a similar coupling of the valence nucleon with the second and third excited states of ^{208}Pb, which are a modestly collective 5^- level and a quite pure particle-hole 4^- level at 3.198 and 3.475 MeV, respectively, have not been unambiguously identified. Cleary, Stein, and Maurenzig[1] have studied the ^{209}Bi(p,p') reaction. They compare scattered proton spectra obtained with incident bombarding energies on and off the analog resonances in ^{210}Po. As a result they identify a set of 19 levels which they ascribe to the common configuration $(\nu g_{9/2}p_{1/2}{}^{-1},\pi h_{9/2})$ in ^{209}Bi. Their data convincingly show that the shell model description of these levels is a good approximation. On the other hand, weak coupling of the $h_{9/2}$ proton to the 5^- and 4^- ^{208}Pb core states also gives 19 levels of the same spins and with about the same excitation energy. Using this model, direct inelastic proton scattering should excite the ten levels based on the 5^- core state quite strongly and the nine states arising from the 4^- state hardly at all. Indeed, the simple weak coupling model predicts that the cross sections for inelastic scattering to states within a multiplet in ^{209}Bi are proportional to $(2I+1)$, where I is the spin of the excited state, times the corresponding cross section for scattering to the core state in ^{208}Pb,

which is strong for the 5^- and weak for the 4^- states. On this basis Wagner, Crawley, and Hammerstein in a later paper[2] made spin assignments that differed for every level from those of Cleary *et al.* For the 2987-keV level, an in-beam γ study with the ^{208}Pb(^{7}Li,$\alpha 2n\gamma$) reaction by Beene *et al.*[3] confirmed the $\frac{19}{2}$ assignment of Cleary *et al.*[1,4]

Although ^{209}Bi has been studied by nearly every possible reaction amenable to charged-particle spectroscopy, including ^{210}Bi$^m(d,t)$ (Ref. 5) and ^{210}Po(t,α) (Ref. 6) with radioactive targets, much additional information is still needed in order to establish many of the level spins and parities. The level density above 3 MeV excitation energy is so high that charged-particle spectroscopy, even with state of the art resolution, is open to ambiguities. Additional information is provided by the study of γ transitions. The septuplet $3^-\otimes h_{9/2}$ has been investigated by Coulomb excitation.[7,8] The γ decay of 11 excited states was established in ^{208}Pb(^{7}Li,$\alpha 2n\gamma$).[3,9] Studies of ^{209}Bi$(n,n'\gamma)$ and (γ,γ') gave information on high energy ($\gtrsim 1$ MeV) transitions.[10] A study using the ^{208}Pb$(d,2n\gamma)$ reaction revealed a $\frac{1}{2}^+$ isomer at $E_x=2442.8$ keV.[11] All of these experiments are very difficult due to low cross sections and large backgrounds, and therefore the γ decays of only about 20 of the lowest 50 excited states have been reported. Among these, only two transitions have an energy below 800 keV, and hence, very little is known about intramultiplet transitions, and the intermultiplet picture is not complete.

Detailed information about the γ-ray transitions among the states we have mentioned would be of considerable aid in identifying the structure of these states, for well-known reasons. To obtain this information we have studied the γ-ray transitions among states in ^{209}Bi with $E_x<4.143$ MeV, which includes some 50 states. States in ^{209}Bi were populated with the ^{208}Pb$(t,2n)^{209}$Bi reaction. The $(t,2n\gamma)$ reaction is very effective for providing a rather complete picture of γ transitions in a nucleus; indeed, it is the only reaction with a large cross section (~ 1 b, exhausting about 80% of the total reaction cross section) available for studying neutron-rich nuclei like ^{209}Bi.

Standard techniques of γ-ray spectroscopy were used. We measured γ-ray angular distributions, γ-ray excitation functions, and γ-γ-time coincidence distributions. We also made some measurements using the pulsed-beam technique.

In the following text after short sections on the experimental procedures, the level scheme and the γ transitions are discussed in detail. The additional 50 γ-ray transitions that we found, in particular, clarify completely the situation concerning the 19 levels of the $(\nu g_{9/2}p_{1/2}^{-1}\pi h_{9/2})$ configuration.

II. EXPERIMENTAL PROCEDURE

The γ decays of levels in ^{209}Bi populated by the ^{208}Pb$(t,2n\gamma)$ reaction were studied with standard in-beam γ spectroscopy techniques. The experiments were performed at the 3-stage Van de Graaff facility of the Los Alamos National Laboratory (LANL). A variety of solid-state Ge detectors were used, including a pure Ge low-energy photon (LEPS) detector [$E_\gamma \lesssim 500$ keV, $\Delta E=0.5$ keV full width at half maximum (FWHM) at 100 keV], a pure Ge planar detector of 10 cm^3 ($E_\gamma \lesssim 1.8$ MeV, $\Delta E=1.0$ keV at 800 keV), and a 50-cm^3 coaxial Ge(Li) detector ($E_\gamma<4$ MeV, $\Delta E=2.5$ keV at 1.5 MeV).

The dominant reaction with a Pb target is $(t,2n)$ for triton energies above the Coulomb barrier (~ 11 MeV) up to about 14.5 MeV, where $(t,3n)$ starts to compete. The $(t,2n)$ cross section approaches 1 b at maximum, accounting for $>80\%$ of the total reaction cross section. Background from interfering reactions is low, so relatively weak transitions can be studied.

Levels with spins ranging from $\frac{1}{2}$ to $\sim\frac{23}{2}$ were populated. The excitation functions are characteristic of the spins of the populated levels. Low-spin states are strongly favored at low triton energy while higher spins dominate at high energies. Therefore, if several bombarding energies are used, quite complete information on the level scheme can be gathered. On the other hand, (hi,xn) reactions mainly populate states close to the yrast line. Reliable information is available on spins, first of all from the selection rules for γ transitions. Excitation functions and angular distributions were also very meaningful.

The following measurements were performed on targets of metallic Pb enriched to $>98.5\%$ ^{208}Pb:

(1) Excitation functions at 90° with the LEPS and the coaxial detectors. Triton energies were 11, 12, 12.5, 13, 14, 15, and 16 MeV and the target thickness was 10 mg/cm^2. Figures 1 and 2 show spectra taken with the LEPS detector.

(2) Excitation functions at 90° with the planar and the coaxial detectors. Triton energies were 11, 12, 13, 14.5, and 16 MeV and the target thickness was 1 mg/cm^2.

(3) Angular distributions at $E_t=13$ and 16 MeV with a 570-mg/cm^2 target that stopped the beam. The plane of the target was 45° to the beam. Spectra were accumulated with the planar detector at 90°, 120°, 135°, and 147° relative to the beam. Simultaneously, the coaxial detector gathered data at 0°, 30°, 45°, 60°, and 90°. Figure 3 shows 90° spectra from this measurement.

(4) Spectra recorded simultaneously from the reaction and from radioactive sources of ^{57}Co, ^{133}Ba,

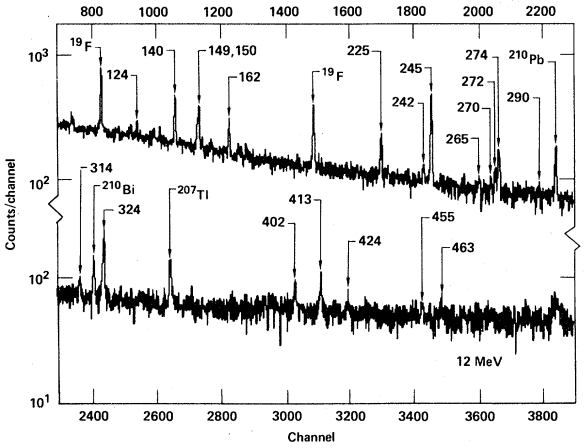

FIG. 1. In-beam γ-ray spectrum from 12-MeV tritons on a thin ^{208}Pb target measured with a LEPS detector. Transitions in ^{209}Bi from the ^{208}Pb$(t,2n)$ reaction are marked by energies in keV. Lines due to other reactions or to impurities are labeled by the nucleus in which they occur.

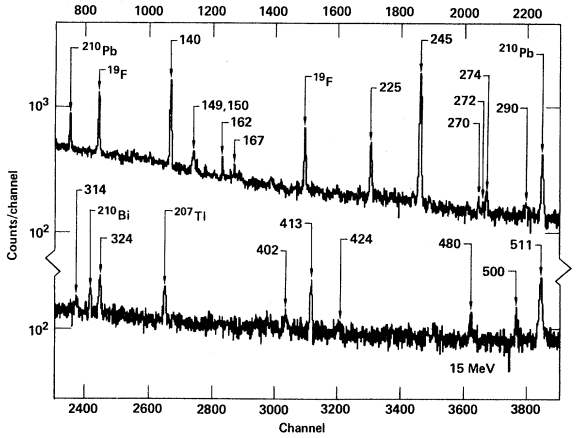

FIG. 2. Same as Fig. 1 but for $E_t = 15$ MeV.

^{137}Cs, ^{54}Mn, ^{60}Co, and ^{24}Na, and alternatively from ^{152}Eu. These data allowed precise energy determinations to be made for the γ transitions in ^{209}Bi.

(5) Coincidences between the two coaxial Ge(Li) detectors at $\pm 90°$ measured with $E_t = 12.5$ and 15 MeV. For each coincident event the energies in both detectors and the time difference between the two γ rays were recorded on tape.

(6) Delayed γ-ray spectra.

III. DATA EVALUATION

Measured spectra are shown in Figs. 1–3. The positions and intensities of the lines were evaluated with the interactive fitting program, FITEK. This program fits sections of the spectrum with a linear background and up to 12 peaks with a Gaussian plus exponential tail simultaneously. The parameters defining the line shape were determined for each energy region from appropriate strong lines. The program gives meaningful errors for peak intensities and positions. Relative detector efficiencies were determined with standard calibration sources, in particular ^{152}Eu, ^{182}Ta, and ^{56}Co. Accurate energy determinations were made with the aid of simultaneous measurements of γ rays from the reaction and from standard sources. These measurements gave precise energy values for about 20 strong γ rays, with errors ranging from 20 eV at 100 keV to 100 eV at 2.7 MeV. All other γ-ray energies were then evaluated relative to these standard transitions. Slight deviations from linearity were taken into account by selecting small sections of the spectrum and sometimes by using second- or third-order polynomials rather than a linear calibration.

Angular distributions were described by the Legendre polynomial,

$$W(\theta) = 1 + A_2 P_2(\cos\theta) + A_4 P_4(\cos\theta) .$$

Table I gives the A_2 coefficients that were determined in the following manner. Least square fits for A_2 only and for A_2 and A_4 were performed on the four sets of data obtained with the planar and coaxial detectors and with $E_t = 13$ and 16 MeV. The planar detector covered the energy range below 1 MeV at $E_t = 16$ MeV and below 2 MeV at $E_t = 13$ MeV. The data were normalized to the isotropic 402- and 1546-keV transitions which depopulate $\frac{1}{2}^+$ states. The observed intensities of low-energy γ rays ($E_\gamma \leq 300$ keV) had to be corrected for absorption in the target. This correction was a function of the detector angle and was calculated from the apparent deviation from isotropy of the Bi K x rays. All results for the A_2 coefficients were compatible, with the exception of a few cases. Particularly, no significant difference between the 13- and 16-MeV data was found. None of the A_4 coefficients differed significantly from zero. The A_2 coefficients and their estimated errors as tabulated are the result of a weighted average of all data. Their errors reflect our estimates of systematic effects and also the possible neglect of a small A_4 term. Table I lists the main properties of all γ transitions in ^{209}Bi that were found in this experiment.

IV. CONSTRUCTION OF THE LEVEL SCHEME

A. General considerations

^{209}Bi has been studied by a large variety of reactions. In particular, inelastic proton scattering ex-

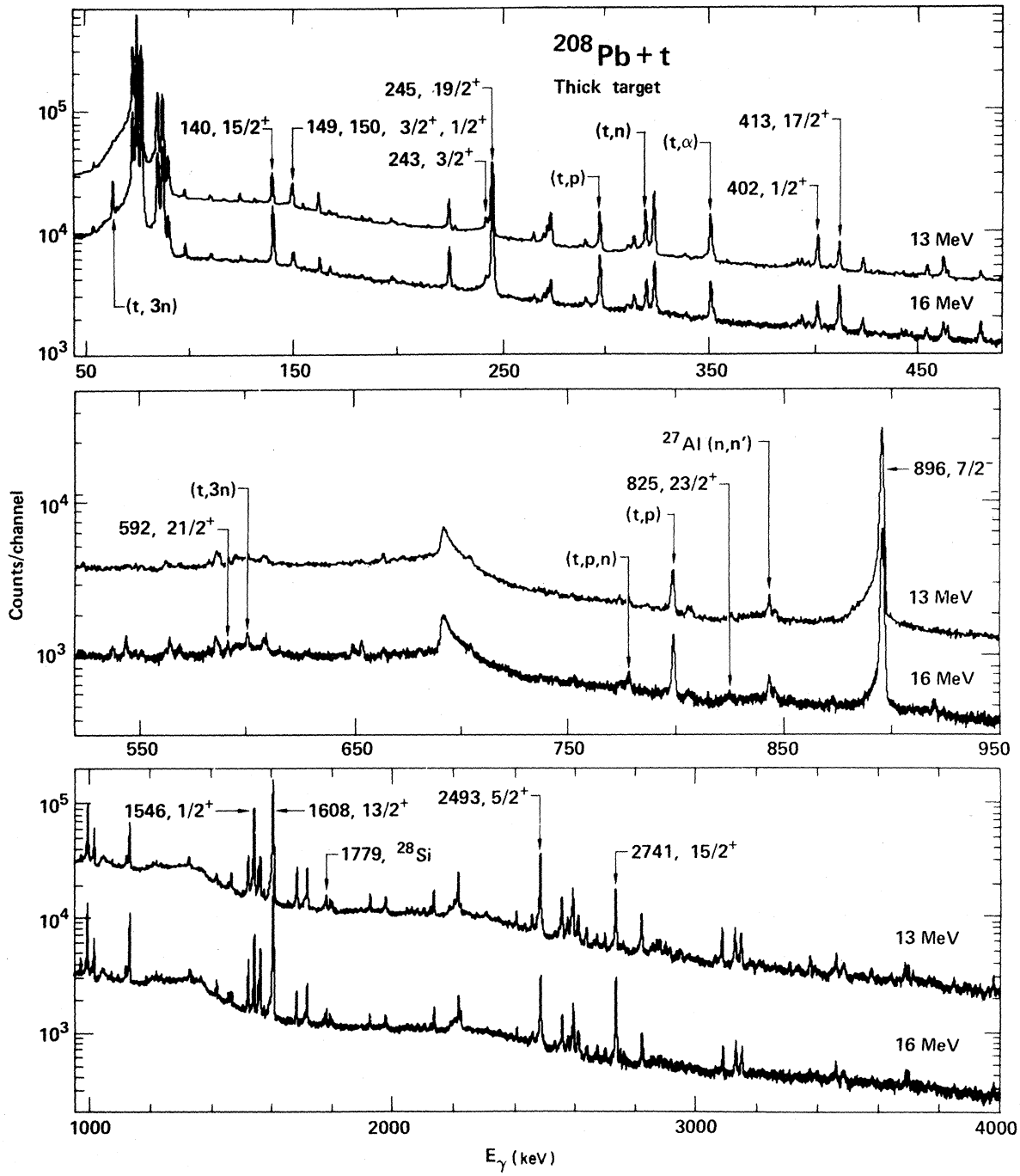

FIG. 3. In-beam γ-ray spectra from a thick ^{208}Pb target bombarded with 13- and 16-MeV tritons. Data below 1 MeV were measured with a planar Ge detector, and those above 1 MeV with a coaxial Ge(Li) diode. Otherwise same as Fig. 1.

periments have established level energies with an accuracy of a few keV.[1,2,4] We therefore assumed that all levels are known in the region of excitation studied in this work ($E \lesssim 4$ MeV) and we tried to assign our observed γ rays to transitions between established levels. New levels were assigned only if this was impossible and if the evidence was compelling. Lines were placed on the basis of the coincidence data and the Ritz principle. In a repetitive procedure precise energies were determined for an increasing number of levels once their decay was established. This reduced the number of possibilities

TABLE I. Gamma transitions in ^{209}Bi from the ^{208}Pb(t,$2n\gamma$) reaction. (D) denotes doublet.

γ energy[a] (keV)	Intensity[a,b] $E_t=13$ MeV	Intensity[a,b] $E_t=16$ MeV	A_2[a,c]	Transition E_i (keV)	Transition E_f (keV)
78.60(10)[d]				(2845	2767)
110.67(15)	0.70(5)	0.70(7)	+0.4(3)	2956	2845
124.48(5)	2.40(6)	1.73(7)	−0.05(5)	2617	2493
131.45(8)	1.06(7)	1.28(7)	0.02(15)	3222	3090
140.13(1)	13.0(2)	38.5(6)	−0.19(4)	2741	2601
149.3(1)	4.8(1)	3.8(2)	−0.08(8)	2767	2617
149.98(5)	9.0(2)	7.1(2)	+0.04(8)	2916	2767
167.16(6)	1.55(8)	3.4(1)	−0.25(10)	3154	2987
225.05(2)	17.3(2)	34.6(5)	−0.15(4)	3212	2987
242.73(5)	6.2(5)			3159	2916
245.73(2)	91(1)	266(5)	+0.31(5)	2987	2741
265.74(8)	4.5(2)	3.7(2)		3222	2956
270.4(1)	4.2(3)	5.5(3)	−0.07(7)	3406	3136
272.2(1)	9.4(2)	8.7(2)	−0.02(4)	3039	2767
273.80(3)	21.4(3)	19.4(3)	+0.02(4)	2767	2493
290.38(10)	3.6(2)	5.7(3)	−0.13(8)	3502	3212
313.70(16)	1.6(5)	7.8(8)		3468	3154
314.2(2)	7.5(6)	6.1(8)	−0.15(10)	3159	2845
323.74(2)	64(1)	61(1)	−0.08(4)	2767	2443
338.65(10)	2.6(2)	2.6(3)	−0.1(2)	2956	2617
352.30(8)	6.1(3)	7.0(3)	+0.03(5)	3197	2845
392.56(10)	4.1(2)	4.4(3)	+0.07(10)	3159	2767
394.72(7)	5.1(2)	11.8(3)	+0.12(8)	3136	2741
402.27(3)	30.1(4)	26.8(4)	0 norm.	2845	2443
413.04(3)	22.5(4)	51.6(8)	−0.32(3)	3154	2741
424.49(8)[(D)]	10.6(3)	13.2(4)	+0.14(3)	3270	2845
				3579	3154
443.15(12)		4.1(3)	−0.1(2)	3597	3154
455.02(10)	11(2)	7.5(3)	−0.12(10)	3222	2767
463.04(8)	18.3(4)	16.6(4)	0.00(5)	2956	2493
480.87(5)	9.0(3)	28.6(6)	+0.43(4)	3468	2987
500.12(5)	7.6(4)	35.3(7)	+0.42(4)	3487	2987
544.85(10)		15.9(5)	−0.23(7)	4142	3597
588.1(4)	10.0(5)	10.3(6)	+0.05(8)	3355	2767
592.2(1)	5.5(5)	10.5(6)	−0.36(12)	3579	2987
610.33(15)		22.3(7)	+0.49(7)	3597	2987
654.98(10)		17.8(7)	−0.28(8)	4142	3487
664.8(2)	9.0(5)	9.4(6)	−0.25(10)	3703	3038
806.36(15)	5.7(6)			3406	2599
825.45(15)		13.8(7)	+0.36(7)	3812	2987
896.30(7)	1000(10)	1000(10)	+0.04(2)	896	0
992.34(2)	112(2)	225(3)	+0.27(1)	2601	1608
1132.45(2)	76(1)	180(2)	−0.12(1)	2741	1608
1524.1(3)	9.6(7)		−0.04(10)	3133	1608
1527.02(8)	49(1)	87(1)	−0.06(2)	3136	1608
1546.47(5)	214(1)	196(2)	0 norm.	2443	896
1560.48(2)	36.0(5)	44(5)	+0.18(5)	3169	1608
1608.48(8)	580(5)	1000(6)	+0.42(1)	1608	0
1686.52(10)	53(1)	46.8(8)	+0.08(2)	2583	896
1720.95(10)	47(1)		−0.04(4)	2617	896
1784.8(2)	14.6(5)	16.2(5)	−0.21(4)	3393	1608
1797.4(2)	11.6(5)	16.0(5)	+0.23(4)	3406	1608
1929.7(2)	16(4)	15(4)		2827	896

TABLE I. (*Continued.*)

γ energy[a] (keV)	Intensity[a,b] $E_t=13$ MeV	Intensity[a,b] $E_t=16$ MeV	A_2[a,c]	Transition E_i (keV)	Transition E_f (keV)
2142.52(15)	32.5(5)	34(3)	−0.07(3)	3039	896
2194.3(2)	7.3(6)		+0.10(12)	3090	896
2223.23(10)	61(1)	65(2)	+0.09(5)	3120	896
2414.85(3)	19.2(6)	16.9(6)	+0.03(5)	3311	896
2465.7(4)		13.0(7)	−0.01(10)	3362	896
2481.7(4)				3378	896
2492.72(10)	171(2)	170(10)	+0.04(2)	2493	0
2553.9(6)	5.9(6)		+0.10(17)	3450	896
2564.3(2)	65(2)	65(2)	+0.25(3)	2564	0
2582.7(4)	23.6(10)	20.4(10)	+0.20(5)	2583	0
2593.5(3)	14(3)	12(3)		3490	896
2599.9(2)	75(1)	89(2)	−0.11(4)	2600	0
2617.25(15)	27(3)	19(4)		2617	0
2645.3(3)	17(1)		+0.05(5)	3542	896
2679.4(4)	20(4)	29(5)		3576	896
2705.5(2)	11.0(5)	22(5)	−0.29(8)	3602	896
2740.99(7)	112(1)	266(2)	+0.48(1)	2741	0
2826.3(2)	52(1)	46(1)	+0.17(5)	2826	0
2887.3(4)	13.9(7)	12.0(7)	+0.17(10)	3784	896
3090.2(2)	41(1)	33(1)	+0.10(5)	3090	0
3132.85(2)	34(1)	36(1)	−0.24(4)	3133	0
3153.2(2)	40(2)	37(1)	+0.26(5)	3153	0
3378.3(4)	15.5(7)	13.5(7)	+0.10(5)	3378	0
3464.0(3)	13.9(6)	13.3(8)	−0.28(8)	3464	0
3491.0(5)	6(2)			3491	0
3693.0(5)	8(2)			3693	0
3703.4(6)	8(2)			3703	0
3719(2)	4(1)			3719	0
3853(2)	4(1)			3853	0
3979.5(6)	10(2)		−0.05(10)	3980	0

[a]Numbers in parentheses are the errors in the least significant digits.

[b]Intensities are the relative thick target yields integrated over all angles, for triton energies of 13 and 16 MeV, respectively.

[c]A_2 is the usual angular distribution coefficient (see text).

[d]This line was detected only with the LEPS detector; its intensity is $\sim 15\%$ of the 402-keV intensity.

for placement of the observed γ rays and in the end a consistent description evolved. The values given in Table II for level energies and their errors were calculated from the γ-ray energies by a least square fit that considers all sequences of transitions between a given level and the ground state, including links through higher-lying states. The errors in Table II therefore reflect the uncertainties in level energies but not necessarily in the energy differences between levels.

Several other requirements were checked when placing a γ ray. Observed γ rays were assumed to have $E1$, $M1$, or $E2$ multipolarities, except for the previously known high-energy $E3$ transitions. This implies that the spin change for a transition has to be $\Delta I \leq 2$. The branching ratio of γ rays depopulating the same level must be independent of the triton energy. This allowed a valuable check for the 13- and 16-MeV angular distribution data. The angular distribution has to be consistent with the assigned spins. Angular distributions follow the usual pattern[12] found in $(hi,xn\gamma)$ reactions. For spins $\geq \frac{13}{2}$ they are quite pronounced, with the observed $A_2 > 0.5A_{2\max}$, where $A_{2\max}$ is the coefficient calculated for a fully aligned nucleus. For low spins the alignment is small. Finally, the spins have to be

TABLE II. Energy levels and γ-ray branching ratios, and multipolarities in ^{209}Bi populated by the ^{208}Pb($t,2n\gamma$) reaction.

Level energy (keV)			γ decay				Final state	
This work[a]	Previous[b]	Spin/parity	E_γ (keV)	Branching ratio (%) This work[c]	Previous[b]	Multipolarity[d]	(keV)	J^π
0	0	$\frac{9}{2}^-$						
896.32(6)	896.4(2)	$\frac{7}{2}^-$	896	100	100	$M1/E2$[e]	0	$\frac{9}{2}^-$
1608.53(6)	1608.48(8)	$\frac{13}{2}^+$	1608	100	100	$M2/E3$[e]	0	$\frac{9}{2}^-$
2442.81(6)	2442.8(5)[f]	$\frac{1}{2}^+$	1546	100	100[f]	$E3$[f]	896	$\frac{7}{2}^-$
2492.75(6)	2492(1)	$\frac{3}{2}^+$	2492	80(10)[g]	100		0	$\frac{9}{2}^-$
			50	20(10)[g]			2443	$\frac{1}{2}^+$
2564.3(2)	2564.51(21)	$\frac{9}{2}^+$	2564	100	100	$E1$[h]	0	$\frac{9}{2}^-$
2582.84(11)	2583	$\frac{7}{2}^+$	2582	31(2)	33(3)	$E1/M2$	0	$\frac{9}{2}^-$
			1686	69(2)	67(3)	$E1/M2$	896	$\frac{7}{2}^-$
2599.77(17)	2599(1)	$\frac{11}{2}^+$	2599	100	85[i]	$E1$	0	$\frac{9}{2}^+$
			991	0(5)	15[i]		1608	$\frac{13}{2}^+$
2600.85(6)	2601(1)	$\frac{13}{2}^+$	992	100	99[i]	$M1/E2$[e]	1608	$\frac{13}{2}^+$
				<5	1	$E3$[e]	0	$\frac{9}{2}^-$
2617.24(7)	2617(1)	$\frac{5}{2}^+$	2617	35(4)	41(4)		0	$\frac{9}{2}^-$
			1720	62(3)	59(4)		896	$\frac{7}{2}^-$
			124	3.1(2)			2493	$\frac{3}{2}^+$
2740.98(6)	2741.07(11)	$\frac{15}{2}^+$	2741	56(1)	56(3)	$E3$	0	$\frac{9}{2}^-$
			1132	37(1)	37(3)	$M1/E2$[e]	1608	$\frac{13}{2}^+$
			140	7(1)		$M1$[j]	2601	$\frac{13}{2}^+$
2766.55(5)	2766(2)	$\frac{3}{2}^+$	324	72(1)		$M1$	2443	$\frac{1}{2}^+$
			274	23.5(5)			2493	$\frac{3}{2}^+$
			149	4.9(4)			2617	$\frac{5}{2}^+$
2826.18(15)	2822(1)	$\frac{5}{2}^-$	2826	76(4)	60	$E2$	0	$\frac{9}{2}^-$
			1930	24(6)	40		896	$\frac{7}{2}^-$
2845.08(7)	2847(4)	$\frac{1}{2}^+$	402	85(10)			2443	$\frac{1}{2}^+$
			(79	15(10))			2767	$\frac{3}{2}^+$
2916.50(7)	2919(4)	$\frac{1}{2}^+$	150	100			2767	$\frac{3}{2}^+$
2955.80(8)	2956(3)	$\frac{3}{2}^+$	463	84(3)			2493	$\frac{3}{2}^+$
			339	12(1)			2617	$\frac{5}{2}^+$
			(111	3.5(5))			2845	$\frac{1}{2}^+$
2986.72(6)	2986(1)	$\frac{19}{2}^+$	246	100	100	$E2$[e]	2741	$\frac{15}{2}^+$
3038.78(10)	3038(2)	$\frac{5}{2}^+$	2143	78(1)		$E1$	896	$\frac{7}{2}^-$
			272	22(1)			2767	$\frac{3}{2}^+$
3090.12(10)	3091(3)	$\frac{7}{2}^+$	3090	100		$E1/M2$	0	$\frac{9}{2}^-$
3119.55(12)	3118(2)	$\frac{3}{2}^-$	2223	100	>95	$E2$	896	$\frac{7}{2}^-$
3132.8(2)		$\frac{11}{2}^+$	3133	78(2)	62[i]	$E1$	0	$\frac{9}{2}^-$
	3135(4)		1524	22(2)	38[i]		1608	$\frac{13}{2}^+$

TABLE II. (*Continued.*)

Level energy (keV)			γ decay				Final state	
			E_γ	Branching ratio (%)		Multi-		
This work[a]	Previous[b]	Spin/parity	(keV)	This work[c]	Previous[b]	polarity[d]	(keV)	J^π
3135.63(8)		$\frac{15}{2}^+$	1527	89(5)		$M1$	1608	$\frac{13}{2}^+$
			395	11(5)		$M1$	2741	$\frac{15}{2}^+$
3153.2(2)		$\frac{9}{2}^+$	3153	100		$E1$	0	$\frac{9}{2}^-$
	3154(4)							
3153.99(6)		$\frac{17}{2}^+$	413	93.5(5)		$M1/E2$	2741	$\frac{15}{2}^+$
			167	6.3(3)		$M1$	2987	$\frac{19}{2}^+$
3159.21(8)		$\frac{3}{2}^+$	393	25(3)			2767	$\frac{3}{2}^+$
			314	40(5)		$M1$	2845	$\frac{1}{2}^+$
			243	35(5)			2916	$\frac{1}{2}^+$
3169.0(2)	3168(2)	$\frac{13}{2}^+$	1560	100	100	$M1$	1608	$\frac{13}{2}^+$
3197.38(15)	3197(10)[k]	$\frac{1}{2}^+, \frac{3}{2}^+, (\frac{5}{2}^+)$	352	100			2845	$\frac{1}{2}^+$
3211.77(7)	3211(1)	$\frac{17}{2}^+$	225	100			2987	$\frac{19}{2}^+$
3221.56(9)	3222(4)	$\frac{5}{2}^+$	455	64(2)			2767	$\frac{3}{2}^+$
			266	28(2)			2956	$\frac{3}{2}^+$
			131	8(2)			3090	$\frac{7}{2}^+$
3269.57(10)		$\frac{1}{2}^+, \frac{3}{2}^+, (\frac{5}{2}^+)$	424	100			2845	$\frac{1}{2}^+$
3311.2(3)	3309(3)	$(\frac{7}{2}^+)$	2415	100			896	$\frac{7}{2}^-$
3354.7(4)	3358(2)	$(\frac{3}{2}^+)$	588	100			2767	$\frac{3}{2}^+$
3362.0(4)	3363(4)	$(\frac{5}{2}^+, \frac{7}{2}^+, \frac{9}{2}^+)$	2466	100			896	$\frac{7}{2}^-$
3378.15(30)	3379(4)	$\frac{9}{2}^+$	3378	>90	100	$E1$	0	$\frac{9}{2}^-$
			(2482)	<10			896	$\frac{7}{2}^-$
3393.3(2)	3393(4)	$(\frac{15}{2}^+)$	1785	100		$M1$	1608	$\frac{13}{2}^+$
3406.07(8)	3406(4)	$\frac{13}{2}^+$	1797	54(3)	100	$M1$	1608	$\frac{13}{2}^+$
			806	27(3)			2600	$\frac{11}{2}^+$
			270	20(2)			3136	$\frac{15}{2}^+$
3450.2(6)	3450(4)	$\frac{7}{2}^+$	3450	0	100		0	$\frac{9}{2}^-$
			2554	100			896	$\frac{7}{2}^-$
3464.0(3)	3466(2)	$\frac{11}{2}^+$	3464	100		$E1$	0	$\frac{9}{2}^-$
3467.60(7)	3469(5)[c]	$\frac{19}{2}^+$	481	81(4)		$M1$	2987	$\frac{19}{2}^+$
			314	19(4)		$M1$	3154	$\frac{17}{2}^+$
3486.85(2)		$\frac{19}{2}^+$	500			$M1$	2987	$\frac{19}{2}^+$
3490.3(2)	3489(4)	$(\frac{7}{2}^+, \frac{9}{2}^+)$	3490	30(15)			0	$\frac{9}{2}^-$
			2594	70(15)			896	$\frac{7}{2}^-$
3502.15(12)	3502(3)	$\frac{15}{2}^+$	290	100		$M1$	3212	$\frac{17}{2}^+$

TABLE II. (*Continued.*)

Level energy (keV) This work[a]	Previous[b]	Spin/parity	E_γ (keV)	γ decay Branching ratio (%) This work[c]	Previous[b]	Multipolarity[d]	Final state (keV)	J^π
3541.6(3)	3543(3)	$(\frac{5}{2}^+, \frac{7}{2}^+, (\frac{9}{2}^+)$	2645	100			896	$\frac{7}{2}^-$
3578.7(3)	3579(3)	$\frac{21}{2}^+$	592	50(20)		$M1$	2987	$\frac{19}{2}^+$
			424	50(30)			3154	$\frac{17}{2}^+$
3597.01(12)	3597	$\frac{19}{2}^+$	610	84(4)		$M1$	2987	$\frac{19}{2}^+$
			443	16(2)			3154	$\frac{17}{2}^+$
3601.8(2)	3603(5)	$(\frac{9}{2}^+)$	2706	100		$E1$	896	$\frac{7}{2}^-$
	3633(4)	$(\frac{1}{2}^-)$						
	3670		3670		100		0	$\frac{9}{2}^-$
	3685(3)							
3693.0(5)	3692(5)	$(\frac{11}{2}^-)$	3693	100			0	$\frac{9}{2}^-$
3703.4(6)	3703(4)	$(\frac{7}{2}^+)$	3703	50(15)			0	$\frac{9}{2}^-$
			665	50(15)		$M1$	3038	$\frac{5}{2}^+$
3719.6(4)	3719(5)	$(\frac{7}{2}^+, \frac{9}{2}^+, (\frac{11}{2}^+)$	3719	100			0	$\frac{9}{2}^-$
3783.6(4)		$(\frac{5}{2}^+, \frac{7}{2}^+, (\frac{9}{2}^+)$	2887	(100)			896	$\frac{7}{2}^-$
3812.17(16)	3815(2)	$\frac{23}{2}^+$	825	100		$E2$	2987	$\frac{19}{2}^+$
3853(2)	3855(3)	$(\frac{7}{2}^+, \frac{9}{2}^+, (\frac{11}{2}^+)$	3853	100			0	$\frac{9}{2}^-$
3979.5(6)	3981(3)	$(\frac{7}{2}^+, \frac{9}{2}^+, (\frac{11}{2}^+)$	3979	100			0	$\frac{9}{2}^-$
4142.84(12)		$\frac{21}{2}^+$	655	53(3)		$M1$	3487	$\frac{19}{2}^+$
			545	47(3)		$M1$	3597	$\frac{19}{2}^+$

[a]Level energies derived from a least-square fit involving all relevant γ-ray cascades.
[b]Reference 10, unless otherwise specified.
[c]From angular distribution data at $E_t = 13$ and 16 MeV integrated over all angles.
[d]Multipolarities are somewhat tentative. They are based solely on the angular distributions and on the spin/parity assignments. A double entry, such as $M1/E2$, means that the angular distribution could not be fitted by a pure multipole of the lowest allowed order. Unique (single) assignments are indicated only if the angular distribution was satisfactorily fitted by the lowest allowed multipolarity.
[e]Reference 10.
[f]Reference 11.
[g]Includes internal conversion.
[h]Reference 9.
[i]Previously unresolved doublet.
[j]Based on our observed γ-ray intensity and the total conversion coefficent required by data in Ref. 3.
[k]Reference 13.

consistent with the excitation function data.

It has been possible to identify all lines having an intensity of at least 1% of the 896-keV transition. As indicated in Figs. 1–3, the reactions (t,α), (t,p), (t,d) or (t,pn), and $(t,3n)$ compete with the $(t,2n)$ reaction. Transitions originating from these reactions were identified by their energies, coincidences, and the excitation function. Also, some γ rays from light elements, particularly ^{19}F and ^{27}Al, appear in the spectra. They are due either to the (n,n') reaction or to some scattered tritons that hit the target chamber. These background lines were much weaker with the thick target that stopped the beam, and they could be identified by unreasonable angular distributions and excitation functions as well as by the absence of coincidences with any transitions in ^{209}Bi.

Table II gives the level scheme as constructed in accordance with the above criteria. Some of the more difficult assignments are discussed in the next section.

B. Detailed assignments of certain levels and transitions

2600-keV doublet. The doublet of states with spins $\frac{11}{2}^+$ and $\frac{13}{2}^+$ at 2600 keV is well known but has not been resolved (Fig. 7). Hertel *et al.*[7] tentatively claimed to see transitions at ~992 keV from the $\frac{11}{2}^+$ and $\frac{13}{2}^+$ levels to the 1608-keV state in Coulomb excitation, but stated that the line from the $\frac{11}{2}^+$ level might be an impurity. Our results allow the determination of energies of both levels in two independent ways, namely by transitions populating and depopulating them. This gives 2599.77(17) keV for the $\frac{11}{2}^+$ and 2600.85(6) keV for the $\frac{13}{2}^+$ level. The spectra with ~1-keV resolution then clearly excluded a 991-keV transition from the $\frac{11}{2}^+$ state.

3135-keV doublet. Based on high strength in the (p,p') reaction both Wagner *et al.*[2] and Cleary *et al.*[1] proposed a doublet at 3135 keV. The γ-ray branching ratio from the $(n,n'\gamma)$ reaction is

$$I(3132\text{ keV}):I(1524\text{ keV})=38:62$$

(Ref. 10). We have clearly resolved 1524-keV and 1527-keV transitions in coincidence with the 1608-keV γ ray, which verifies that two levels exist. In addition, the lower state decays to the ground state and the higher to the $\frac{15}{2}^+$ level at 2741 keV. The latter decay is clearly established from coincidences with the 2741-keV transition. Therefore a change of the intensity ratio

$$I(1527\text{ keV})/I(395\text{ keV})$$

by 20% between the 13- and 16-MeV data is discarded as being due to some other interfering small line. The decay of the level at 3132.8 keV to $\frac{9}{2}^-$ and $\frac{13}{2}^+$ states and the angular distributions of these transitions require a spin of $\frac{11}{2}$ for the 3132.8-keV state. Likewise, a spin of $\frac{15}{2}$ is required for the 3135.6-keV level. This agrees with the assignments of Cleary *et al.*[1] based on analog resonances, while the tentative spins $\frac{13}{2}^+$, $\frac{19}{2}^+$ of Wagner *et al.*[2] are rejected.

3154-keV doublet. Again, the strength in (p,p') studies and resonances at the $4^-,5^-$ and $8^-,9^-$ analog states suggested a doublet with spins of $\frac{9}{2}^+$ and $\frac{17}{2}^+$ assigned by Cleary *et al.*,[1] while Wagner *et al.*[2] proposed $\frac{7}{2}^+$ and $\frac{15}{2}^+$. Transitions of 1544 and 3152 keV have been assigned to this level from $(n,n'\gamma)$ (Ref. 10) and (^{7}Li,$\alpha 2n\gamma$) studies.[9] Our coincidence data exhibit no evidence of a 3154→1608→0 cascade. It is highly probable that the earlier conclusions resulted from a misinterpretation of the 1546-keV line from the 2443-keV level. We find a 3153-keV transition with an angular distribution that strongly favors $E1$ with $\Delta J=0$. The 3154-keV member of the doublet decays to $\frac{15}{2}^+$ and $\frac{19}{2}^+$ levels and both γ rays have angular distributions that are compatible with $M1$ transitions from a $\frac{17}{2}^+$ state. In addition, this state is populated from a $\frac{19}{2}^+$ level. In summary, our data require a doublet with spins $\frac{9}{2}^+$ and $\frac{17}{2}^+$.

New low-spin levels. Low-spin states decay preferentially through the $\frac{1}{2}^+$ level at 2443 keV. Gamma rays from low-spin states are thus in coincidence with the 1546- and 896-keV cascade γ rays from this $\frac{1}{2}^+$ level to the ground state. In both Figs. 4(a) and (c), the spectra in coincidence with the 896- and 1546-keV γ rays, respectively, exhibit a 324- and a 402-keV transition. We placed these lines as transitions from previously known levels at 2767 keV ($\frac{3}{2}^+$) and 2845 keV ($\frac{1}{2}^+$) to the 2443-keV level.

Figure 4(d) shows the spectrum in coincidence with the 402-keV transition that depopulates the 2845-keV $\frac{1}{2}^+$ state. Transitions of 314, 352, and 424 keV are evident, in addition to the 896- and 1547-keV lines from the decay of the 2443-keV level. We place the 352-keV γ ray as deexciting a level at 3197 keV. A level is reported at this energy in the ^{207}Pb$(\alpha,d)^{209}$Bi reaction.[13] The spectrum in coincidence with the 424-keV γ ray shows clear γ-ray peaks of 402, 1546, and 896 keV. Therefore the 424-keV transition clearly deexcites a new level at 3270 keV. However, the 424-keV peak is also in coincidence with the 413-keV γ ray which depopulates the level at 3154 keV. This implies that the 424-keV line is a doublet and that the second component connects the 3579- and 3154-keV levels. At

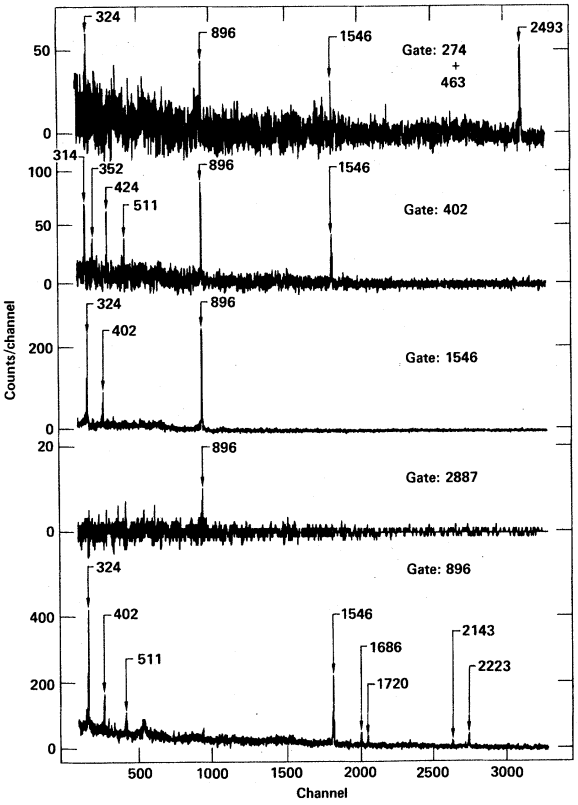

FIG. 4. γ-γ coincidences in ^{208}Pb$(t,2n)^{209}$Bi measured at $E_t=12.5$ MeV. The spectra are coincidences with: (a) the 896-keV line, (b) 2887 keV, (c) 1546 keV, (d) 402 keV, and (e) sum of 274 and 463 keV. Energies (keV) of transitions are indicated.

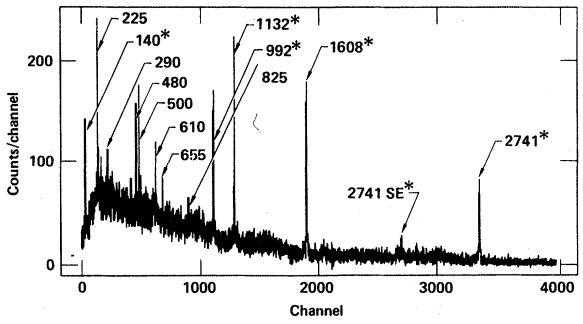

FIG. 5. Coincidences with the 245-keV transition in ^{208}Pb$(t,2n)^{209}$Bi at $E_t=15$ MeV. Energies (keV) of lines are indicated. Transitions marked by an asterisk follow the 245-keV transition; all others precede it.

314 keV there is another doublet that is not resolved in the coincidences. In this case the excitation functions clearly show that the 314.2-keV line comes from a low-spin state while the 313.7-keV line depopulates a high-spin state. For the 3159-keV level depopulated by the 314.2-keV transition, two more decays have been found that are also proven by coincidences.

High-spin states. The decay of high-spin states proceeds mainly through the $\frac{19}{2}^+$ level at 2987 keV. This state decays via a 245-keV transition to the $\frac{15}{2}^+$ 2741-keV level. Figures 5 and 6(a) show the spectrum in coincidence with the 245-keV γ ray. Transitions marked by an asterisk are due to the decay of the 2741-keV state. Other peaks in Figs. 5 and 6(a) at 225, 480, 500, 610, and 825 keV, and a weak peak at 592 keV, are from γ rays that populate the $\frac{19}{2}^+$ 2987-keV state. The 500-keV transition is preceded by a 655-keV line and the 610-keV transition by a 545-keV line as shown in Figs. 6(b)–(d). The energy sums $655+500$ and $610+545$ are equal within experimental errors, the difference being (80 ± 200) eV. This indicates there is a level at 4142 keV that decays via two parallel cascades. The angular distributions give $A_2(500)=+0.42(4)$ and $A_2(610)=+0.49(7)$ as

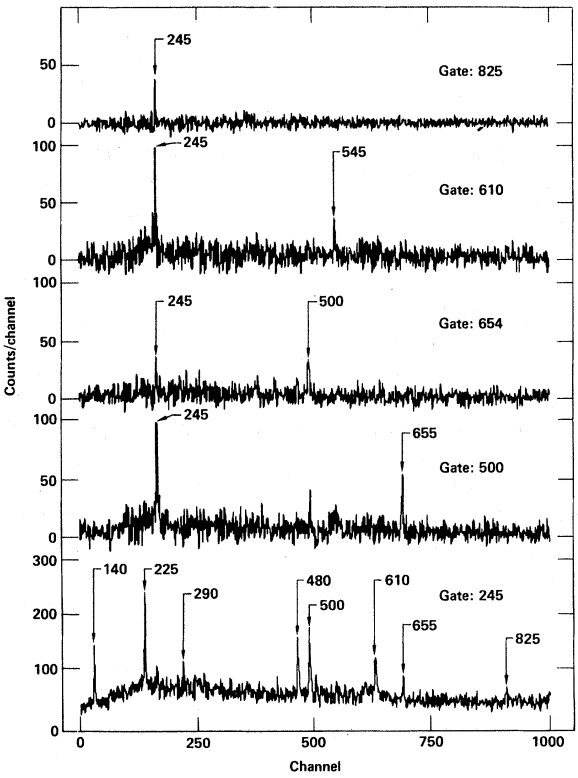

FIG. 6. γ-γ coincidences in ^{208}Pb$(t,2n)^{209}$Bi measured at $E_t=15$ MeV. The spectra are in coincidence with the following lines: (a) 245, (b) 500, (c) 654, (d) 610, and (e) 825 keV. Energies of transitions are indicated.

compared to the predictions[12]

$$A_2(\tfrac{23}{2}(E2)\tfrac{19}{2}) \leq 0.40$$

and

$$A_2(\tfrac{19}{2}(M1)\tfrac{19}{2}) \leq 0.50 .$$

The transitions from the 4142-keV level have $A_2(545) = -0.23(7)$ and $A_2(655) = -0.28(8)$ while $A_{2\max}(\tfrac{21}{2}(M1)\tfrac{19}{2}) = -0.29$. A sequence of $\tfrac{21}{2}^+(M1)\tfrac{19}{2}^+(M1)\tfrac{19}{2}^+$ for both cascades is the only reasonable assignment. Negative parities can be excluded on the basis of structure arguments that will be discussed later.

The angular distribution of the 825-keV γ ray has $A_2 = +0.36(7)$, which implies a stretched $E2$ transition. Therefore the 3812-keV level, which is firmly established from coincidences [Figs. 6(a) and (e)], has spin $\tfrac{23}{2}^+$, which is the highest spin found in this experiment. The assignments of the 480- and 592-keV γ rays to levels at 3468 and 3578 keV are confirmed by other transitions from these levels which are firmly placed by coincidences. The spins of these two states are also well established. It should be noted that Cleary, Stein, and Maurenzig[1] found that the ^{209}Bi(p,p') reaction populated an $\tfrac{11}{2}^+$ level at 3465 keV; Cleary, Callender, and Sheline[5] found an $l=3$ transition to a level of the same energy that was populated by the (d,t) reaction on 3.0×10^6-y ^{210}Bi^m ($J^\pi = 9^-$), which implies a spin of $J \geq \tfrac{13}{2}$. Their suggestion of a doublet is clearly verified since our data confirm the $\tfrac{19}{2}^+$ state at 3468 keV, and also show a 3464-keV γ ray with the correct angular distribution for $\tfrac{11}{2}^+(E1)\tfrac{9}{2}^-$.

Further remarks. The data available for placement of high-energy γ rays from the high-lying states above 3.2 MeV that decay only to the ground state are very limited, since there are no coincidences to confirm the placements. Entries in the table of levels therefore mean that we are convinced from the variety of spectra taken that these transitions occur in ^{209}Bi. They therefore were assigned as ground-state transitions from the closest previously known level. All the decays to the 896-keV state on the other hand are proven by coincidences. As an example, the spectrum in coincidence with the 2887-keV line is shown in Fig. 4(b).

V. DISCUSSION OF THE LEVEL SCHEME AND THE GAMMA TRANSITIONS

A. Single-proton states

The single-proton states have been well established by proton transfer to ^{208}Pb. We see the decays of the $f_{7/2}$, $i_{13/2}$, $f_{5/2}$, and $p_{3/2}$ levels at 896, 1608, 2826, and 3120 keV, respectively. The assignments are clear and agree with previous work, except for the branching ratio in the decay of the $f_{5/2}$ state. Many new γ-ray transitions were found that populate the $h_{9/2}$ ground state and the $f_{7/2}$ and $i_{13/2}$ states, while no discrete γ rays were seen populating the $f_{5/2}$ and $p_{3/2}$ states.

B. Two-proton—one-proton-hole states

Proton particle-hole excitations of the ^{208}Pb core lie, in general, above the corresponding neutron p-h excitations. Therefore we cannot expect to see two-proton—one-proton-hole states. An exception is the levels of the structure (^{210}Po g.s., π^{-1}). The strong pairing interaction in the 0^+ ground state of ^{210}Po lowers these levels by about 1 MeV.

The ^{210}Po(t,α) (Ref. 6) reaction identified the $s_{1/2}$ hole state at 2.43 MeV and the $h_{11/2}{}^{-1}$ level at 3.69 MeV. It also disclosed a splitting of the $d_{3/2}$ hole strength between levels at 2.48 and 2.95 MeV. Ellegaard *et al.*[11] studied the ^{208}Pb$(d,n\gamma)$ reaction and found an isomer at 2.443 MeV which is the $\tfrac{1}{2}^+$ state in ^{209}Bi. They extensively discuss the isomeric decay by an $E3$ transition to the $\tfrac{7}{2}^-$ 896-keV level and confirm the $(s_{1/2}{}^{-1}\otimes{}^{210}\text{Po})$ structure of the $\tfrac{1}{2}^+$ state. Our results on the isomeric decay agree with this interpretation. The spin assignment $\tfrac{1}{2}^+$ is further strengthened beyond any doubt by many transitions populating this level. Configuration mixing of this state with the ^{208}Pb $5^-\otimes h_{9/2}$ level will be discussed.

Cleary *et al.* identified the $^{210}\text{Po}\otimes d_{3/2}{}^{-1}$ configuration with the 2493- and 2956-keV levels. The 2493-keV level is primarily a member of the ^{208}Pb $3^-\otimes h_{9/2}$ septuplet. However, $l=3$ and $E3$ strength are missing in inelastic scattering and Coulomb excitation experiments, respectively. In both experiments, part of the missing strength is found in the 2956-keV level, thus showing configuration mixing. This mixing is also evident from the γ decay of the 2956-keV level. This level is most strongly deexcited (84% of the total decay rate) by a transition to the 2493-keV level. It also branches to the $\tfrac{5}{2}^+$ member of the septuplet, while no decay ($<3\%$) has been seen to the $(^{210}\text{Po}\otimes s_{1/2}{}^{-1})$ state at 2.443 MeV. Since this latter transition is l forbidden and slow, we do not expect to see it in competition with the observed allowed transitions, even though these allowed transitions proceed through the smaller admixed part of the wave function.

We have tentatively placed a very weak 111-keV transition between the 2956-keV state and the $(^{208}\text{Pb}\ 5^-\otimes h_{9/2})_{(1/2)^+}$ level at 2845 keV. The energy fits

perfectly and there is no other possibility of placing this line in the adopted level scheme. Also, the observed excitation function is reasonable for a low-spin ($\frac{3}{2}^+$) level. The A_2 coefficient has a large error and we cannot expect to see coincidences for this weak low-energy line. If the line is placed correctly then it has the largest transition matrix element of any decay branch from the 2956-keV level. This cannot be easily explained unless there is mixing between the $(5^-\otimes h_{9/2})$ configuration and the proton two-particle one-hole state.

Finally, the $h_{11/2}$ hole state should decay only to the ground state, since it is an allowed $h_{11/2}\rightarrow h_{9/2}$ $M1$ transition. We see a 3693-keV transition that we assign to this decay.

C. The $3^-\otimes\pi h_{9/2}$ septuplet

The levels and transitions that involve the septuplet are shown in Fig. 7. This group of levels has been studied experimentally by inelastic scattering[2,4,14] and by Coulomb excitation.[7,8] Many theoretical models have been used to describe it.[15–22] We will only point out the new information gained in this experiment. The doublet of the $\frac{11}{2}^+$ and $\frac{13}{2}^+$ levels at 2.600 MeV has been clearly resolved and the individual spins have been verified. A tentatively proposed 991-keV transition between the $\frac{11}{2}^+$ 2.6-MeV state and the single-particle $i_{13/2}$ level at 1608 keV is rejected by our data. The branching of the 2741-keV $\frac{15}{2}^+$ state found by Beene *et al.*[3] in the decay of the $\frac{19}{2}^+$ isomer is confirmed. The 140-keV $M1$ transition between the $\frac{15}{2}^+$ and the $\frac{13}{2}^+$ members of the septuplet is clearly evident in our spectra. So far the existence of this transition had been proven only indirectly, though very convincingly.[3] A discrepancy exists, however, in the angular distribution of the 1132-keV transition between the 2741-keV $\frac{15}{2}^+$ and the 1608-keV levels. Beene *et al.*[3] measured A_2 (1132 keV)$=-0.01(5)$ while the present data give consistently at both $E_t=13$ and 16 MeV $A_2=-0.12(1)$. Otherwise, our data agree very well with those of Beene *et al.* Our results would imply less $E2$ admixture, namely $\delta(E2/M1)=+0.05$ as compared to $\delta=+0.14$ in Ref. 3 (with the phase convention of Yamazaki[12] as used throughout).

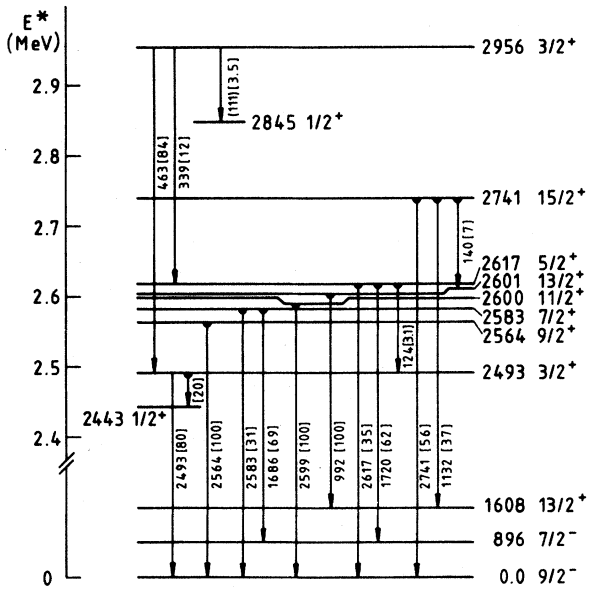

FIG. 7. The $3^-\otimes h_{9/2}$ septuplet. Levels belonging to the septuplet and their γ-ray decay are shown, including the admixed 2956-keV $\frac{3}{2}^+$ state. The indicated branching ratios are for γ-ray decay only except for the 2493-keV state, where internal conversion of the 50-keV transition is included. For transitions into these levels see Fig. 8.

We have already commented on the mixing of the $d_{3/2}$ hole state and the $(3^-\otimes h_{9/2})_{(3/2)^+}$ level. The $M1$ transitions to members of the septuplet provide additional evidence of this mixing. For these transitions the matrix element

$$\langle \pi h_{9/2}||\mathcal{M}(M1)||\pi h_{9/2}\rangle$$

is ~ 2.5 times as large as the

$$\langle 3^-||\mathcal{M}(M1)||3^-\rangle$$

matrix elements. Using only the first matrix element, the γ branching ratio from the 2956-keV $\frac{3}{2}^+$ state to the $\frac{3}{2}^+$ and $\frac{5}{2}^+$ members of the septuplet is calculated as 7. This agrees exactly with the measured ratio and further supports the assignment of a $(3^-\otimes h_{9/2})$ component to the 2956-keV level. The decay to the septuplet is due to this part of its wave function.

Another $M1$ transition, of 124.5 keV, has been placed between the 2617-keV $\frac{5}{2}^+$ and the 2493-keV $\frac{3}{2}^+$ levels. With the same assumptions we can relate its $B(M1)$ value to that of the 140-keV $\frac{15}{2}^+\rightarrow\frac{13}{2}^+$ transition. The result is

$$B(M1,124\text{ keV})/B(M1,140\text{ keV})=1.5\ .$$

From the lifetime and branching of the $\frac{15}{2}^+$ level the partial half-life of the 140-keV γ transition is 120 ps. This gives ~ 120 ps for the 124-keV γ-ray transition. The total half-life of the $\frac{5}{2}^+$ level is >2 ps,[10] hence, a branching $>2\%$ for the 124-keV γ ray is indicated. This agrees with the measured branch of 3.1%. Electron conversion brings the total intensity of this transition up to 15%.

Another low-energy transition that depopulates the 2493-keV $\frac{3}{2}^+$ level can be inferred. The evi-

dence is presented in Fig. 4(e), which shows the spectrum in coincidence with the 274- and 463-keV lines that both populate the 2493-keV state. The occurrence in this spectrum of the 1547-keV line that originates from the 2443-keV level means that a branch of $\sim 20\%$ (including conversion electrons) exists from the 2493 to the 2443-keV level. The half-life of the 2493-keV level is ~ 40 ps.[10] Therefore the partial half-life for the 50-keV transition is 200 ps as compared to the single-particle estimate of 10 ps for $M1$ radiation. The hindrance factor of 20 implies there is little mixing of these states.

The newly discovered γ transitions improve the experimental picture of the $3^- \otimes \pi h_{9/2}$ septuplet. All the spins have been confirmed, in particular those for the previously unresolved $\frac{11}{2}^+, \frac{13}{2}^+$ doublet. The mixing with the ^{210}Po g.s.$\otimes \pi d_{3/2}{}^{-1}$ level is clearly verified by the connecting transitions. The 124- and 50-keV transitions and some changes in branching ratios imply that the Coulomb excitation experiments[7,8] should be reinterpreted.

D. Levels of the $(\nu g_{9/2} p_{1/2}{}^{-1}, \pi h_{9/2})$ configuration

1. General

The lowest two-particle one-hole states in ^{209}Bi are predicted to have the $(\nu g_{9/2} p_{1/2}{}^{-1}, \pi h_{9/2})$ configuration if one considers only the single-particle energies. Only three other two-proton-one-proton-hole states are lower or comparable in energy, due to the strong pairing interaction in the ^{210}Po ground state as discussed previously. This configuration gives a total of 19 levels with spins between $\frac{1}{2}^+$ and $\frac{19}{2}^+$.

Cleary, Stein, and Maurenzig[1] have identified these 19 levels in ^{209}Bi(p,p') inelastic proton scattering through the analog resonances in ^{210}Po of the low-lying levels in ^{210}Bi, which have the structure $(\nu g_{9/2} \pi h_{9/2})$. Their cited article[1] is the main reference for this section. Completely different spins were assigned by direct (p,p') scattering based on a weak coupling interpretation of the data in Ref. 2.

Little other experimental information has been available. Inelastic neutron scattering[10] and ^{208}Pb(^{7}Li,$\alpha 2n\gamma$) (Refs. 3 and 9) gave a few high-energy γ transitions from these levels. The latter reaction clearly verified the $\frac{19}{2}^+$ assignment by Cleary *et al.* since this level is isomeric and could be easily studied. In the present work we were able to find the γ decays of all levels of this configuration. The experimental results are summarized in Fig. 8 and Table III. In the following the level scheme and the transitions are discussed using simplifying assumptions concerning the structure of the levels.

For now we will assume a pure $(\nu g_{9/2} p_{1/2}{}^{-1}, \pi h_{9/2})$ configuration. There are three equivalent coupling schemes:

$$|(\nu g_{9/2} p_{1/2}{}^{-1}) I_1, \pi h_{9/2}; I\rangle \quad \text{with } I_1 = {}^{208}\text{Pb } 4^-, 5^- ,$$

$$|(\nu g_{9/2} \pi h_{9/2}) I_2, \nu p_{1/2}{}^{-1}; I\rangle \quad \text{with } I_2 = {}^{210}\text{Bi } 0^-, \ldots, 9^- ,$$

$$|(\nu p_{1/2}{}^{-1} \pi h_{9/2}) I_3, \nu g_{9/2}; I\rangle \quad \text{with } I_3 = {}^{208}\text{Bi } 4^+, 5^+ .$$

All two-particle matrix elements of the residual interaction as well as the single-particle energies can be taken from experiment. From these the energies and eigenfunctions can be calculated in a straightforward way. (The calculations are as in Ref. 1 which, however, has some misprints in the formula and consistently a wrong phase in the wave functions. See Ref. 15, Vol. 1, p. 73 for the recoupling coefficients.) In Table III the theoretical energies and the eigenfunctions are given. We choose to use the first representation from above, in which we couple the $h_{9/2}$ proton to the 4^- and 5^- core states in ^{208}Pb. Figure 9 shows the energies that are involved. Column 1 gives the unperturbed energy of the $(\nu g_{9/2} p_{1/2}{}^{-1})$ configuration in ^{208}Pb. Column 2 shows the experimental energies of the two ^{208}Pb states that are mainly of this structure. The next two columns show how the $(\nu p_{1/2}{}^{-1} \pi h_{9/2})$ interaction (^{208}Bi) and the $(\nu g_{9/2} \pi h_{9/2})$ interaction (^{210}Bi) affect the energies. Finally, the experimental energies of the lowest and highest states in ^{209}Bi are shown. As can be seen, the 19 levels in ^{209}Bi occur at the predicted energies and are spread out over an energy range approximately equal to the combined effect of the three residual interactions.

The calculated and the experimental energies are compared in Fig. 8. In general the agreement is within ~ 50 keV. We arrive at the same correspondence between experimental and theoretical levels as Cleary *et al.*[1] The only exception is the upper $\frac{3}{2}^+$ level. Cleary *et al.* assigned a 3363-keV level as the $J = \frac{3}{2}$ member of this multiplet. We found a new level at 3159 keV which compares with the theoretical energy of 3172 keV. This state is a much better candidate for the multiplet, as we will show by its γ decay. Furthermore, the level at 3362 keV does not have $J^\pi = \frac{3}{2}^+$, since it decays to the 896-keV $\frac{7}{2}^-$ level. However, a 3355-keV state decays only to the

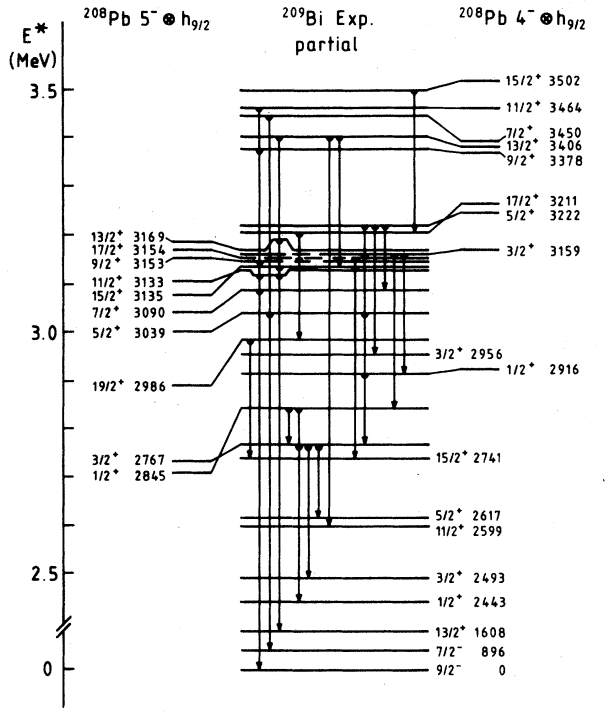

FIG. 8. Levels of the $(\nu g_{9/2}p_{1/2}{}^{-1},\pi h_{9/2})$ configuration and their γ-ray decay. The levels of this configuration are marked by extensions to the left if their main parentage is ^{208}Pb 5^-, to the right if ^{208}Pb 4^-. The positions in the center column and the numbers give the measured energies (keV) while the extensions show energies from a shell model calculation. Other levels are shown only if they are populated by transitions from the multiplet. Note that the three lowest levels are not drawn to scale. See also Table III and the text.

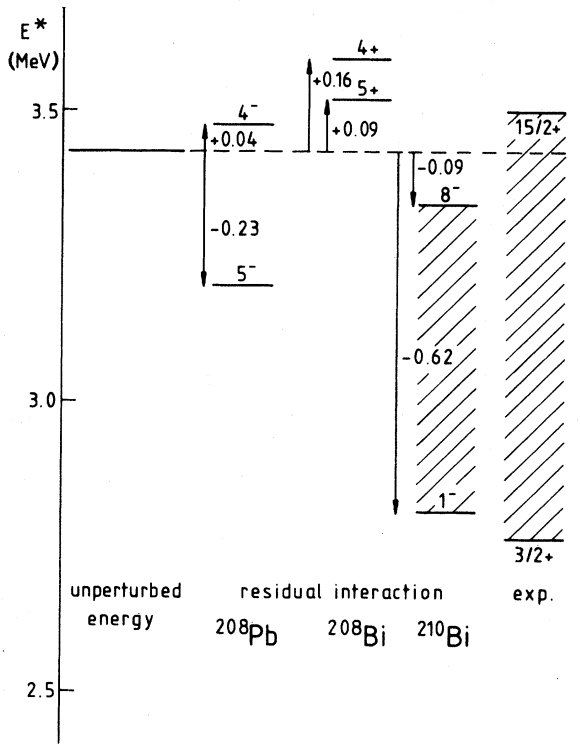

FIG. 9. Relevant energies for the levels of the configuration $(\nu g_{9/2}p_{1/2}{}^{-1},\pi h_{9/2})$ in ^{209}Bi. Column 1 shows the unperturbed excitation energy of this configuration: $E=\Delta(^{207}\text{Pb})+\Delta(^{209}\text{Pb})-2\Delta(^{208}\text{Pb})=3.43$ MeV. The next columns show the deviations of the two particle levels due to the residual interaction, e.g., $\Delta E(^{210}\text{Bi}\ 1^-)=\Delta(^{210}\text{Bi}\ 1^-)+\Delta(^{208}\text{Pb})-\Delta(^{209}\text{Pb})-\Delta(^{209}\text{Bi})$. The last column gives the experimental energies of the multiplet. Only the lowest and highest states are shown. The experimental levels evidently are at the expected energy and spread out over a range comparable with the residual interactions.

$(5^-\otimes h_{9/2})_{(3/2)^+}$ level at 2766 keV. It is very likely that the 3355-keV state and the 2766-keV level are mixed. This would explain why the 3355-keV level decays only to the 2766-keV state while many other transitions are possible. Also, the observations in the inelastic scattering experiment[1] that Cleary *et al.* identified with the

$$|\pi h_{9/2},\nu g_{9/2}p_{1/2}{}^{-1};\tfrac{3}{2}^+\rangle$$

configuration would be explained by this mixed 3355-keV state.

The largest differences between calculated and measured energies occur for the lower $\frac{1}{2}^+$ and the $\frac{19}{2}^+$ states. This can be qualitatively understood. The 5^- state in ^{208}Pb is not a pure particle-hole state of the configuration $(\nu g_{9/2}p_{1/2}{}^{-1})$, but is moderately collective; the second largest component is $(\pi h_{9/2}s_{1/2}{}^{-1})$. For this component the Pauli principle forbids the formation of a $\frac{19}{2}^+$ state with the additional $h_{9/2}$ proton in ^{209}Bi. It also guarantees that

$$|(\pi h_{9/2}s_{1/2}{}^{-1})5^-,\pi h_{9/2};\tfrac{1}{2}^+\rangle = |(\pi h_{9/2}{}^2)0^+,s_{1/2}{}^{-1};\tfrac{1}{2}^+\rangle\ .$$

Therefore the impurity of the 5^- state implies a mixing of the $\frac{1}{2}^+$ level with the

$$|^{210}\text{Po}\ 0^+,s_{1/2}{}^{-1};\tfrac{1}{2}^+\rangle$$

state. For all other levels this admixture in the ^{208}Pb 5^- state has a much smaller effect and the energies agree indeed extremely well. It should also be mentioned that the 1^- ground state of ^{210}Bi is not very pure, while all other levels that were used to determine the two-particle matrix elements are quite pure. We want to point out here that our approach is, of course, not rigorous theoretically. We use, on

TABLE III. Gamma decay from levels of the $(\nu g_{9/2}p_{1/2}^{-1},\pi h_{9/2})$ configuration. Energies (E) are in keV.

Initial state					Final state				Experimental	Theoretical decay
J^π	E_{exp}	E_{th}	$A(5^-)$[a]	$A(4^-)$[a]	J^π	E_{exp}	Main config.[b]	E_γ	branching[c]	rate[d] (10^{12} s^{-1})
$\frac{1}{2}^+$	2845	2708	0.997	0.080	$\frac{3}{2}^+$	2767		79	15(10)	0.037
					$\frac{1}{2}^+$	2443	$h_{9/2}^2 s_{1/2}$	402	85(10)	0.1
					$\frac{3}{2}^+$	2493	$3^-\otimes h_{9/2}$	352	0	10^{-3}
$\frac{1}{2}^+$	2916	2921	0.080	−0.997	$\frac{3}{2}^+$	2767		150	100	0.18
					$\frac{1}{2}^+$	2845		71	0	10^{-3}
					$\frac{3}{2}^+$	2493	$3^-\otimes h_{9/2}$	423	0	0.02
$\frac{3}{2}^+$	2767	2731	0.906	−0.423	$\frac{1}{2}^+$	2443	$h_{9/2}^2 s_{1/2}$	324	72(1)	
					$\frac{3}{2}^+$	2493	$3^-\otimes h_{9/2}$	274	23.5(5)	5×10^{-4}
					$\frac{5}{2}^+$	2617	$3^-\otimes h_{9/2}$	149	4.9(4)	7×10^{-5}
					sum		multiplet			0
$\frac{3}{2}^+$	3159	3172	0.423	+0.906	$\frac{3}{2}^+$	2767		393	25(3)	1.2
					$\frac{1}{2}^+$	2845		314	40(5)	0.77
					$\frac{1}{2}^+$	2916		243	35(5)	1.4
					sum		$3^-\otimes h_{9/2}$			0.05
$\frac{5}{2}^+$	3039	3004	0.991	−0.131	$\frac{3}{2}^+$	2767		272	22(1)	1.6
					$\frac{7}{2}^-$	896	$f_{7/2}$	2143	78(1)	
$\frac{5}{2}^+$	3222	3246	0.131	0.991	$\frac{3}{2}^+$	2767		455	64(2)	1.1
					$\frac{7}{2}^+$	3090		131	8(2)	0.04
					$\frac{3}{2}^+$	2956	$h_{9/2}^2 d_{3/2}$	266	28(2)	
					sum		$3^-\otimes h_{9/2}$			0.07
$\frac{7}{2}^+$	3090	3041	0.960	−0.280	$\frac{5}{2}^+$	3039		51	0	0.01
					$\frac{9}{2}^-$	0	$h_{9/2}$	3090	100	
					sum		$3^-\otimes h_{9/2}$			0.003
$\frac{7}{2}^+$	3450	3392	0.280	0.960	$\frac{7}{2}^-$	896	$f_{7/2}$	2554	100	
					$\frac{5}{2}^+$	3222		228	0	2.3
					sum		$3^-\otimes h_{9/2}$			0.16
$\frac{9}{2}^+$	3153	3155	0.999	0.001	$\frac{9}{2}^+$	0	$h_{9/2}$	3153	100	
					$\frac{7}{2}^+$	3090		63		0.020
					sum		$3^-\otimes h_{9/2}$			10^{-3}
$\frac{9}{2}^+$	3378	3369	0.001	−0.999	$\frac{9}{2}^+$	0	$h_{9/2}$	3378	100	
					$\frac{7}{2}^+$	3090		288		0.24
					$\frac{11}{2}^+$	3133		245		0.41
					sum		$3^-\otimes h_{9/2}$			0.13
$\frac{11}{2}^+$	3133	3106	0.977	−0.214	$\frac{9}{2}^-$	0	$h_{9/2}$	3133	78(2)	
					$\frac{13}{2}^+$	1608	$i_{13/2}$	1524	22(2)	
					sum		multiplet			0
					sum		$3^-\otimes h_{9/2}$			0.002
$\frac{11}{2}^+$	3464	3465	0.214	−0.977	$\frac{9}{2}^-$	0	$h_{9/2}$	3464	100	
					sum		multiplet			0.50
					sum		$3^-\otimes h_{9/2}$			0.18

TABLE III. (*Continued.*)

Initial state					Final state						
J^π	E_{exp}	E_{th}	$A(5^-)$[a]	$A(4^-)$[a]	J^π	E_{exp}	Main config.[b]	E_γ	Experimental branching[c]	Theoretical decay rate[d] (10^{12} s^{-1})
$\frac{13}{2}^+$	3169	3185	0.999	0.051	$\frac{13}{2}^+$	1608	$i_{13/2}$	1560	100	
					sum		multiplet			0.008
							$3^-\otimes h_{9/2}$			$<10^{-3}$
$\frac{13}{2}^+$	3407	3380	0.051	−0.999	$\frac{15}{2}^+$	3136		270	20(2)	0.55
					$\frac{11}{2}^+$	3133		274	0	0.15
					$\frac{11}{2}^+$	2600	$3\otimes h_{9/2}$	806	27(3)	0.1
					$\frac{13}{2}^+$	2601	$3\otimes h_{9/2}$	808	0	0.04
					$\frac{13}{2}^+$	1608	$i_{13/2}$	1797	54(3)	
$\frac{15}{2}^+$	3136	3078	0.985	−0.173	$\frac{15}{2}^+$	2741	$3^-\otimes h_{9/2}$	395	11(2)	$<10^{-3}$
					$\frac{13}{2}^+$	2601	$3\otimes h_{9/2}$	535	0	0.001
					$\frac{13}{2}^+$	1608	$i_{13/2}$	1527	89(2)	
					sum		multiplet			0.
$\frac{15}{2}^+$	3502	3519	0.173	−0.985	$\frac{17}{2}^+$	3212		290	100	1.5
					$\frac{17}{2}^+$	3154		348	0	0.5
					$\frac{13}{2}^+$	2601	$3^-\otimes h_{9/2}$	901	0	0.16
$\frac{17}{2}^+$	3154	3171	0.835	0.550	$\frac{19}{2}^+$	2987		167	6.3(3)	0.06
					$\frac{15}{2}^+$	2741	$3^-\otimes h_{9/2}$	413	98.5(5)	0.006
$\frac{17}{2}^+$	3212	3264	0.550	−0.835	$\frac{19}{2}^+$	2987		225	100	0.45
					$\frac{15}{2}^+$	2741	$3^-\otimes h_{9/2}$	471	0	0.02
$\frac{19}{2}^+$	2987	2892	1.0	0.0	$\frac{15}{2}^+$	2741	$3^-\otimes h_{9/2}$	246	(τ=26 ns $E2$)	

[a]These are the amplitudes of the model wave function: $A(5^-)\,|\,^{208}\text{Pb}\ 5^-,\pi h_{9/2};I> + A(4^-)\,|\,^{208}\text{Pb}\ 4^-,\pi h_{9/2};I\rangle$.
[b]Multiplet means levels of the $(\nu g_{9/2}p_{1/2}^{-1},\pi h_{9/2})$ configuration.
[c]From Table II. All transitions found experimentally are listed.
[d]See text. Only the two or three strongest decays predicted by theory are listed.

one hand, the shell model, and we assume that the states contain only one configuration. On the other hand, experimental matrix elements are employed which definitely include effects of configuration mixing. The idea is that the known insufficiencies of the shell model without configuration mixing are, by and large, compensated by using experimental numbers that already contain higher-order corrections.

2. *Gamma-ray transitions*

In this subsection the measured transitions associated with levels of the $(\nu g_{9/2}p_{1/2}^{-1},\pi h_{9/2})$ configuration are compared with calculations. The calculations are again simple; they take into account only the major features, relying completely on experimental information from neighboring nuclei.

We consider only $M1$ transitions within the multiplet. Both $M1$ and $E2$ transitions proceed with about single-particle strength. For γ energies of less than 500 keV the $M1$ transitions are then about 2 to 3 orders of magnitude faster than $E2$ transitions. Also, experimentally, many $M1$ transitions are found while no clear evidence for $E2$ transitions exists. We choose again the representation based on the ^{208}Pb 5^- and 4^- states. The contributions to the total $M1$ transition strength are sketched as:

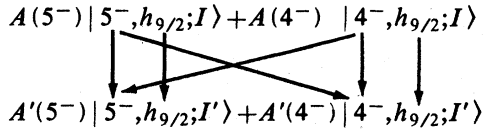

The arrows indicate the possible transitions. The to-

tal transition matrix element can be calculated following, e.g., Bohr and Mottelson (Ref. 15, Vol. 1, p. 84, Eqs. (1a)–(72a)]. The four transition elements in units of μ_N are derived from experiments as:

$$\langle h_{9/2}||\mathcal{M}(M1)||h_{9/2}\rangle = +7.02(7)\ ,$$

$$\langle 5^-||\mathcal{M}(M1)||5^-\rangle = +0.27(15)\ ,$$

$$\langle 4^-||\mathcal{M}(M1)||4^-\rangle = -2.9(2)\ ,$$

$$\langle 4^-||\mathcal{M}(M1)||5^-\rangle = +1.2(4)\ .$$

The $h_{9/2}\rightarrow h_{9/2}$ and $5^-\rightarrow 5^-$ elements are calculated [Eqs. (3)–(40), p. 337 of Ref. 15, Vol. 1) from the measured magnetic moments

$$\mu(^{209}\mathrm{Bi}^g) = 4.11\ \mu_N$$

and

$$\mu(^{208}\mathrm{Pb}\ 5^-) = +0.15\ \mu_N$$

(Ref. 23). The magnetic moment of the ^{208}Pb 4^- level is not known. Its wave function is, however, very pure $(\nu g_{9/2} p_{1/2}{}^{-1})$ and we can reliably calculate $(^{208}\mathrm{Pb}\ 4^-) = -1.77\ \mu_N$ from the measured single-particle moments $\mu(\nu g_{9/2}) = -1.33\ \mu_N$ (Ref. 24) and

$$\mu(\nu p_{1/2} = \mu(^{207}\mathrm{Pb\ g.s.}) = 0.58\ \mu_N$$

(Ref. 23). The transition rate of the $4^-\rightarrow 5^-$ transition is measured[23] and gives the transition matrix element as $\pm 1.2\ \mu_N$. A calculation assuming pure $(\nu g_{9/2} p_{1/2}{}^{-1})$ configurations based on the cited single-particle moments gives $+1.6\ \mu_N$, in good agreement with the experiment, and fixes the sign. In this way all the parameters required to calculate the transition rates between levels of the $(\nu g_{9/2} p_{1/2}{}^{-1}, \pi h_{9/2})$ configuration are obtained from experimental data.

One discrepancy inherent to this approach is the following. The measured moment of the 5^- level is $+0.15(5)\ \mu_N$. This has to be compared with

$$\mu(\nu g_{9/2} p_{1/2}{}^{-1}; 5^-) = -0.75\ \mu_N$$

as determined from the single-particle moments. The discrepancy is once more mainly due to the neglect of the $(\pi h_{9/2} s_{1/2}{}^{-1})$ component of the 5^- level with a magnetic moment of $\sim +6\ \mu_N$. Fortunately, the $5^-\rightarrow 5^-$ matrix element occurs only with the $\pi h_{9/2}\rightarrow\pi h_{9/2}$ transition element and is $\sim\frac{1}{25}$ as large; hence it can be regarded as a minor correction.

Another significant mode of decay is to the $3^-\otimes h_{9/2}$ septuplet. In this case the $5^-\rightarrow 3^-$ $E2$ transition in the ^{208}Pb core is negligible compared with the contribution due to the $4^-\rightarrow 3^-$ $M1$ transition. The half-life of the $5^-\rightarrow 3^-$ $E2$ transition in ^{208}Pb is 0.29 ns and the transition energy is 583 keV, while the half-life of the 4^- level is 4 ± 3 ps.[23] After a correction for branching the partial half-life of the 860-keV $4^-\rightarrow 3^-$ $M1$ transition is 7 ± 5 ps. For a typical transition energy in ^{209}Bi of 500 keV the half-life due to the $4^-\rightarrow 3^-$ $M1$ transition is therefore 35 ps as compared to 625 ps for the $5^-\rightarrow 3^-$ $E2$ transition. This factor of 18 is the reason for taking into account only the $4^-\rightarrow 3^-$ $M1$ element. In short, we calculated

$$A(5^-)\,|\,5^-, h_{9/2}; I\rangle + A(4^-)\,|\,4^-, h_{9/2}; I\rangle$$
$$\downarrow\ (M1)$$
$$|\,3^-, h_{9/2}; I'\rangle\ .$$

The recoupling of the angular momenta has been handled properly. The transition rates are proportional to $E_\gamma{}^3$, $A^2(4^-)$, and the $4^-\rightarrow 3^-$ $M1$ decay rate in ^{208}Pb. Typical $B(M1)$ values for transitions to the septuplet are $\lesssim 0.01\ \mu_N{}^2$ as compared to $\gtrsim 1\ \mu_N{}^2$ for the $M1$ transitions between levels within the multiplet. For spins ranging from $\frac{5}{2}^+$ to $\frac{11}{2}^+$, $E1$ decay to the $\frac{9}{2}^-$ ground state or the $\frac{7}{2}^-$ 896-keV level is also possible with γ energies of 2 to 3 MeV. The single-particle estimate in this case gives $t_{1/2} < 10^{-16}$ s, but these $E1$ transitions are highly forbidden. The same holds for $M1$ transitions to the $i_{13/2}$ state at 1608 keV, for which the single-particle estimate gives $t_{1/2} \approx 10^{-14}$ s. The allowed $M1$ transitions between the $(\nu g_{9/2} p_{1/2}{}^{-1}, \pi h_{9/2})$ states are often slow or virtually impossible due to the low energies involved. So we often have the interesting situation that all decay modes are hindered by structure or energy and thus small impurities of the wave functions become decisive.

3. *Comparison of experimental and model calculations*

The measured and calculated γ decay properties are compared in Table III.

$\frac{1}{2}^+$ states. The lower $\frac{1}{2}^+$ state decays to the

$$|\,(\pi h_{9/2}{}^2, 0^+), s_{1/2}{}^{-1}; \tfrac{1}{2}^+\rangle$$

level. This is understandable from the $(\pi h_{9/2} s_{1/2}{}^{-1})$ component of the 5^- level in ^{208}Pb. The quoted decay rate of $10^{11}\ \mathrm{s}^{-1}$ has been calculated for a 10% admixture in the 5^- core state and by using $\mu(\pi s_{1/2}) = 1.8\ \mu_N$.[25] A weak transition of 78.6 ± 0.1 keV, seen only with the LEPS detector, might be the expected branch to the 2767-keV $\frac{3}{2}^+$ state. Its excitation function agrees with that of the main 402-keV decay branch within the rather large error. The upper $\frac{1}{2}^+$ level decays only to the 2767-keV $\frac{3}{2}^+$ state of the same configuration, in accor-

dance with theory. The absence of a transition to the 2443-keV level, as found for the lower $\frac{1}{2}^+$ state, implies that the upper $\frac{1}{2}^+$ state has little 5^- parentage and that the 4^- core state contains little of the $(\pi h_{9/2} s_{1/2}^{-1})$ configuration. The transition energy would favor this unobserved decay mode by a factor of 30 over the observed transition.

$\frac{3}{2}^+$ states. The 2767-keV level is the lowest of the 19 levels considered here. It therefore has to decay to states of different structure. The branching ratio to the $\frac{3}{2}^+$ and $\frac{5}{2}^+$ levels of the $(3^-\otimes h_{9/2})$ septuplet agrees with the theoretical estimate. The main decay mode to the 2443-keV level ($E_\gamma = 324$ keV) is not covered by our simple model. The predicted decay rates to the septuplet are very small. If they are realistic, the unexplained 324-keV transition has a strength of 10^{-3} single-particle units.

The $\frac{3}{2}^+$ level at 3159 keV decays with about equal γ-ray intensities to the lower $\frac{3}{2}^+$ and both $\frac{1}{2}^+$ levels. This is very close to the prediction of the model wave functions. In this case we can deduce the wave functions of the $\frac{1}{2}^+$ and $\frac{3}{2}^+$ levels from the measured branching ratios. The two unknown quantities are the mixing ratios in the $\frac{1}{2}^+$ and $\frac{3}{2}^+$ levels at 2845 and 2767 keV, respectively. They are uniquely determined by the intensities of two transitions normalized to the third. The wave functions have been calculated in this way. For

$$|\tfrac{3}{2}^+, 2767 \text{ keV}\rangle = 0.95\,|5^-, h_{9/2}\rangle - 0.3\,|4^-, h_{9/2}\rangle$$

and

$$|\tfrac{1}{2}^+, 2845 \text{ keV}\rangle = 0.94\,|5^-, h_{9/2}\rangle + 0.35\,|4^-, h_{9/2}\rangle\ ,$$

the calculated branching ratios are the following: $\frac{3}{2}^+$ 2767: 27(6), $\frac{1}{2}^+$ 2845: 40(6), and $\frac{1}{2}^+$ 2916: 32(6). This is in complete agreement with the measurement. The errors given for the calculated branchings reflect the uncertainties of the $M1$ matrix elements. It should be pointed out that the overlap integrals between the wave functions calculated from the Hamiltonian and those determined from the branching ratios are 0.99 for the $\frac{3}{2}^+$ levels and 0.97 for the $\frac{1}{2}^+$ levels, a remarkable agreement.

Cleary *et al.*[1] designated a level at 3354 keV to be the $(4^-, h_{9/2}; \frac{3}{2}^+)$ state (see also Sec. V F). In their experiment the 3159 keV-level is buried by the much stronger 3154-keV doublet and the 3170-keV line. However, the transition to the 3170-keV state shows a resonance at the 2^- analog state, which with regard to the results from the γ transitions, has to be interpreted as due to the $\frac{3}{2}^+$ 3159-keV level. Nevertheless, the (p,p') work indicates that the 3354-keV level may have some of the $(4^-, h_{9/2}; \frac{3}{2}^+)$ strength.

$\frac{5}{2}^+$, $\frac{7}{2}^+$, and $\frac{9}{2}^+$ states. The levels with spins $\frac{5}{2}^+$ through $\frac{11}{2}^+$ can decay by $E1$ transitions of 2 to 3 MeV to the $\frac{9}{2}^-$ ground state or the $\frac{7}{2}^-$ level at 896 keV. The single-particle estimate gives lifetimes of $\sim 10^{-17}$ s for these transitions. On the other hand, these $E1$ decays are forbidden. The competition between the allowed $M1$ decays with typically $t_{1/2} = 10^{-12}$ s and the $E1$ transitions is a stringent test for the purity of the wave functions. The lower $\frac{5}{2}^+$ level shows both types of decays, implying a hindrance of the $E1$ transition of 10^4. For the higher $\frac{5}{2}^+$ level at 3222 keV no high-energy transition has been seen. It decays to the two levels of the same configuration for which the model gives the fastest decay rates, although the branching disagrees with the model by a factor of 3. The additional transition to the 2956-keV level having the main structure (^{210}Po g.s., $d_{3/2}^{-1}$) might indicate that the 3222-keV level contains a (^{210}Po g.s., $d_{5/2}^{-1}$) component. For the $\frac{7}{2}^+$ and $\frac{9}{2}^+$ levels the $E1$ transitions dominate. However, the allowed $M1$ decays are also predicted to be very weak for the lower levels of both spins.

$\frac{11}{2}^+$ and $\frac{13}{2}^+$ levels. These levels can decay by fast $M1/E2$ transitions to the $i_{13/2}$ single-particle level at 1608 keV. For the lower levels of both spins the allowed $M1$ decays within the multiplet are predicted to be very weak and we see only high-energy transitions. The upper $\frac{13}{2}^+$ level exhibits three decay branches. The ratio of intensities to the $(5^-, h_{9/2}; \frac{15}{2}^+)$ and $(3^-, h_{9/2}; \frac{11}{2}^+)$ levels is close to the predictions. Failure to observe the expected transition to the $\frac{11}{2}^+$ state at 3133 keV might be due to another γ ray at this energy (see Table I). The $i_{13/2}$ single-particle state is populated most strongly.

$\frac{15}{2}^+$ to $\frac{19}{2}^+$ levels. The $\frac{19}{2}^+$ state at 2987 keV can only be formed by the $(5^-\otimes h_{9/2})$ configuration. Due to its low energy it can only decay to the $\frac{15}{2}^+$ member of the septuplet at 2741 keV. The mean life is 26 ns and this isomer has been well studied.[3] The $\frac{17}{2}^+$ and $\frac{15}{2}^+$ levels exhibit decay patterns that agree approximately with predictions. However, both the $\frac{15}{2}^+$ and the $\frac{17}{2}^+$ levels at 3136 and 3154 keV, respectively, decay more strongly than expected to the $(h_{9/2}\otimes 3^-; \frac{15}{2}^+)$ level. A small mixing ($\sim 10\%$) of the 2741-keV and 3136-keV $\frac{15}{2}^+$ levels would account for this; the competing decay modes are very weak in both cases. The higher-lying $\frac{15}{2}^+$ and $\frac{17}{2}^+$ states were observed to decay only by the branch that is predicted theoretically to be strongest.

4. *Summary of the* $(\nu g_{9/2}p_{1/2}^{-1}\pi h_{9/2})$ *configuration*

The combined results of inelastic proton scattering[1,4] and the present study of γ transitions have definitely identified the 19 levels of the $(\pi h_{9/2},\nu g_{9/2}p_{1/2}^{-1})$ configuration. A shell-model calculation using empirical matrix elements is reasonably successful in reproducing the measured energies and γ-ray branching ratios. Mixing with other configurations is evident for the $\frac{1}{2}^+$, $\frac{3}{2}^+$, and $\frac{19}{2}^+$ levels. The use of matrix elements as measured in neighboring nuclei is extremely helpful for revealing the main structure of the levels and for establishing the correspondence between experimental and theoretical levels. We are aware of only one calculation of these levels, that by Zawischa.[17] He estimates that his approach using the Migdal theory should give the energies of the $5^-\otimes h_{9/2}$ decuplet within a few keV if the interaction parameters are correct. A comparison of Zawischa's results with experiment is given in Fig. 10. The agreement is indeed good, within 100 keV, except for the $\frac{1}{2}$ and $\frac{3}{2}$ levels and the $\frac{5}{2}$ state based on the 4^- core state. This calculation therefore runs into difficulties for the same levels as does the empirical shell model. While the Migdal theory takes into account many more configurations, the basic input data are the same as for the shell model. In particular, the neutron-proton interaction, that contributes most to the splitting of the multiplets, is in both cases taken from the ^{210}Bi level scheme. Zawischa does not calculate transition rates.

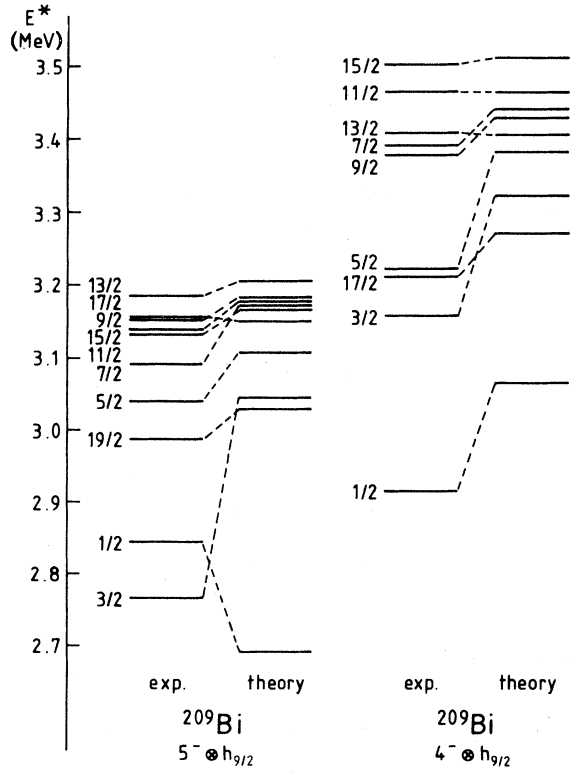

FIG. 10. Comparison of experimental level energies of the $5^-\otimes h_{9/2}$ and $4^-\otimes h_{9/2}$ multiplets with the calculation by Zawischa (Ref. 17).

Iwasaki, Ring, and Schuck[22] calculated the decuplet and nonet using Dyson's boson expansion. They achieved good agreement for the energies of the levels that belong to the 5^- core state. In particular, the $\frac{3}{2}^+$ and $\frac{1}{2}^+$ states are well reproduced. The energies of the nonet states do not fit quite as well, and transition rates for comparison have not been calculated.

E. High-spin states

The results on high-spin states are summarized in Fig. 11. We also show the results of a ^{210}Bi$^m(d,t)$ experiment[5] that selectively populates levels consisting of a neutron hole coupled to the $(\nu g_{9/2},\pi h_{9/2};9^-)$ level of ^{210}Bi. The column marked Theory shows the energies of the highest spin members of the indicated configurations as calculated with experimentally determined two-particle interaction energies.[26] The lowest three levels have been discussed in the previous section.

$\frac{23}{2}^+$ level. Coincidences between the 826-keV γ

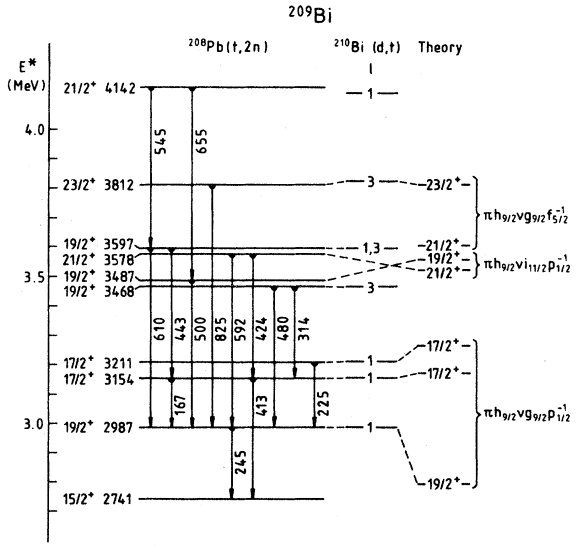

FIG. 11. High-spin levels in ^{209}Bi. Levels with spin $\geq\frac{17}{2}$ as established in this experiment and their γ decay are shown. For comparison corresponding states seen in ^{210}Bi$^m(d,t)$ and the transferred angular momentum are given. On the right calculated levels are indicated; the upper four levels are from Ref. 25.

ray that populates the 2987-keV $\frac{19}{2}^+$ level and the 246-keV γ ray that depopulates it clearly establish this level [Figs. 6(a) and (e)]. The angular distribution of the 826-keV line shows this transition to be a stretched $E2$ and determines the 3812-keV state to have $J^\pi=\frac{23}{2}^+$. There is only one low-lying configuration that gives $\frac{23}{2}^+$, namely an $f_{5/2}$ neutron hole coupled to the 9^- state in ^{210}Bi. The measured and calculated energies[26] agree perfectly. The ^{210}Bi$^m(d,t)$ reaction also populates a level with $l=3$ at this energy. Furthermore, the most favorable decay mode is the single-particle $E2$ transition $f_{5/2}\rightarrow p_{1/2}$ that is indeed found experimentally.

$\frac{19}{2}^+$ and $\frac{21}{2}^+$ levels. Our understanding of these states is not clear. The expected lowest-lying high-spin levels of the $(\pi h_{9/2},\nu i_{11/2}p_{1/2}^{-1})$ and $(\pi h_{9/2},\nu g_{9/2}f_{5/2}^{-1})$ configurations do not correspond well with the experimental level scheme. In particular three levels with spin $\frac{19}{2}^+$ have been found at $\sim$3.5 MeV while only one is expected; the $(\pi h_{9/2}\nu g_{9/2}f_{5/2}^{-1};\frac{19}{2}^+)$ state should be above the $\frac{21}{2}^+$ state at 3.6 MeV. The (d,t) experiment[5] shows that the $l=1$ strength is split between the 3987- and 3597-keV states and the $l=3$ strength is distributed between the latter and the 3468-keV level. This indicates considerable configuration mixing. Cleary *et al.*[4] also found in (p,p') that $l=5$ strength is missing in the $\frac{19}{2}^+$, 2986-keV level and suggested that the missing strength is found in the 3597-keV state. We tentatively identify the 3487- and 3578-keV levels with the $(\pi h_{9/2},\nu i_{11/2}p_{1/2}^{-1})$ configuration, since they are not present in the (d,t) experiment. It is not certain if the $\frac{21}{2}^+$ level at 4142 keV can be identified with the (4122±10)-keV state that is excited by pickup of a $p_{3/2}$ neutron in ^{210}Bi$^m(d,t)$. For a $p_{3/2}$ hole, an allowed $M1$ transition to the corresponding $p_{1/2}$ hole state at 2987 keV should dominate, but it is absent in the experiment. We might conclude that the structure of the high-spin states is characterized by appreciable configuration mixing and therefore the gamma transitions cannot be easily explained. The measurements give, however, firm spin assignments by which shell model calculations can be tested.

F. Levels of unknown structure

The previous discussions left out 14 levels seen in this experiment about which little is known. These states are listed in Table IV. All levels belonging to the ^{208}Pb $(3^-,5^-,4^-)\otimes h_{9/2}$ configurations have been found. The next expected multiplets are $3^-\otimes f_{7/2}$ at an unperturbed energy of 3.5 MeV and $5_2^-\otimes h_{9/2}$ at 3.7 MeV. They split, respectively,

TABLE IV. Levels of unknown structure in ^{209}Bi. Energies are in keV. Spin/parity assignments are discussed in the text.

Level energy	E_γ	Branching ratio	Final state	Tentative spin
3197.38(15)	352		2845 $\frac{1}{2}^+$	$\frac{1}{2}^+,\frac{3}{2}^+,(\frac{5}{2}^+)$
3269.57(10)	424		2845 $\frac{1}{2}^+$	$\frac{1}{2}^+,\frac{3}{2}^+,(\frac{5}{2}^+)$
3311.2(3)	2415		896 $\frac{7}{2}^-$	$(\frac{7}{2}^+,\frac{9}{2}^+)$
3354.7(4)	588		2767 $\frac{3}{2}^+$	$(\frac{3}{2}^+)$
3362.0(4)	2466		896 $\frac{7}{2}^-$	$(\frac{5}{2}^+,\frac{7}{2}^+,\frac{9}{2}^+)$
3393.3(2)	1785		1608 $\frac{13}{2}^+$	$(\frac{15}{2}^+)$
3490.3(2)	3490	30(15)	0 $\frac{9}{2}^-$	$(\frac{7}{2}^+,\frac{9}{2}^+)$
	2594	70(15)	896 $\frac{7}{2}^-$	
3541.6(3)	2645		896 $\frac{7}{2}^-$	$(\frac{5}{2}^+,\frac{7}{2}^+,\frac{9}{2}^+)$
3601.8(2)	2706		896 $\frac{7}{2}^-$	$(\frac{9}{2}^+)$
3703.4(6)	3703		0 $\frac{9}{2}^-$	$(\frac{7}{2}^+)$
	(665		3038 $\frac{5}{2}^+$)	
3719.6(4)	3719		0 $\frac{9}{2}^+$	$(\frac{7}{2}^+,\frac{9}{2}^+,\frac{11}{2}^+)$
3783.6(4)	2887		896 $\frac{7}{2}^-$	$(\frac{5}{2}^+,\frac{7}{2}^+,\frac{9}{2}^+)$
3853(2)	3853		0 $\frac{9}{2}^-$	$(\frac{7}{2}^+,\frac{9}{2}^+,\frac{11}{2}^+)$
3979.5(6)	3979		0 $\frac{9}{2}^-$	$(\frac{7}{2}^+,\frac{9}{2}^+,\frac{11}{2}^+)$

into seven levels with spins from $\frac{1}{2}^+$ to $\frac{13}{2}^+$ and ten levels with spins from $\frac{1}{2}^+$ to $\frac{19}{2}^+$. Zawischa[17] calculated the energies of these states in Migdal theory. He finds that the $3^-\otimes f_{7/2}$ multiplet extends from 3.25 to 3.76 MeV and the $5_2^-\otimes h_{9/2}$ multiplet from 3.35 to 3.75 MeV. Since little is known experimentally about spins we cannot compare experiment and theory. As already seen for the high-spin states, strong configuration mixing is likely for the levels at ~3.5-MeV excitation energy. The only firm theoretical prediction is that only positive-parity states occur. All the low-lying levels in ^{208}Pb have negative parity, and the two lowest orbitals for the additional protons in Bi, $h_{9/2}$ and $f_{7/2}$, also have negative parity.

The tentative spin assignments in Table IV are based on this assumption of positive parity and on the restriction that only $E1$, $M1$, and $E2$ transitions compete. This limits the spin of a state decaying to the $\frac{9}{2}^-$ ground state or the $\frac{7}{2}^-$ first excited state within $\pm 1\hbar$. The parity-changing $M2$ or $E3$ transitions should, of course, be much slower. It should be understood that this procedure gives only the most reasonable estimates of the spins.

The two new low-spin levels at 3197 and 3269 keV probably have spin $\frac{1}{2}^+$ or $\frac{3}{2}^+$. For the same reasons as discussed in Sec. V D, $E2$ transitions should be much weaker than $M1$. This makes $J^\pi=\frac{5}{2}^+$ improbable for these levels. Also, $\frac{5}{2}^+$ levels could decay to many more levels, including the $\frac{7}{2}^-$, 896-keV state. Cleary *et al.*[1,4] gave $\frac{7}{2}^-$ for the 3311-keV state since (p,p') resonates at the 4^- analog resonance. This agrees with the γ decay which, however, does not rule out $\frac{9}{2}^+$.

The 3355 and 3362 levels have not previously been resolved. One of these levels has to be the $\frac{3}{2}^+$ state that was observed in the (p,p') reaction and was assumed to belong to the $(\pi h_{9/2},\nu g_{9/2}p_{1/2}{}^{-1})$ configuration.[1] While, as shown in Sec. V D, a better candidate for this has been found, the 3355-keV state must contain some of this configuration. The γ transition to the 2767-keV $(5^-\otimes h_{9/2})_{(3/2)^+}$ state supports this conclusion. The 3362-keV level is $\frac{5}{2}^+$, $\frac{7}{2}^+$, or $\frac{9}{2}^+$ by our general arguments.

Most angular distributions are not very pronounced and are subject to large errors due to the small intensities. The 3393→(1608 keV, $\frac{13}{2}^+$) γ ray of 1785 keV has $A_2=-0.21(4)$. This is typical for ($I\rightarrow I-1$, $M1$, or $E1$). Therefore this level has $I=(\frac{15}{2}^+)$. The 2706-keV transition from the 3602-keV level to the 896-keV $\frac{7}{2}^-$ level shows a similar angular distribution with $A_2=-0.29(8)$. For this parity-changing transition, $\frac{9}{2}^+\rightarrow\frac{7}{2}^-$, $E1$ is strongly favored over $\frac{7}{2}^+\rightarrow\frac{7}{2}^-$, $M2$. The 665-keV line with $A_2=-0.25(10)$ could not be uniquely assigned to the level at 3703 keV. However, if our assignment is correct, the angular distribution of the 665-keV γ ray and the branch to the ground state require a spin/parity of $\frac{7}{2}^+$ for the 3703-keV state. For all other levels in Table IV no information, other than the selection rules governing γ-ray transitions and the structure argument for positive parity, is available for use in assigning spins.

VI. CONCLUSIONS

In-beam γ-ray spectroscopy with the ^{208}Pb$(t,2n\gamma)$ reaction has revealed many new γ-ray transitions in ^{209}Bi. The good energy resolution of germanium diodes gave level energies with one to two orders of magnitude higher precision than charged-particle work has previously provided. In turn some doublets could be clearly resolved and new levels established. The selection rules for γ-ray transitions and the angular distributions have also led to many firm spin assignments.

For the $3^-\otimes h_{9/2}$ septuplet the mixing of the 2493-keV $\frac{3}{2}^+$ level with the (^{210}Po g.s., $d_{3/2}{}^{-1}$) state at 2956 keV has been verified by γ-ray transitions. Also, a new branch from the 2493-keV state to the (^{210}Po g.s., $s_{1/2}{}^{-1}$) level and an $M1$ transition between the $\frac{5}{2}^+$ and $\frac{3}{2}^+$ members of the multiplet have been found. The significance of these findings is that the septuplet is the standard text book example for particle-vibration coupling, and that it is very often used to test new theoretical approaches.

The main result of this experiment concerns the 19 levels from the $(\pi h_{9/2},\nu g_{9/2}p_{1/2}{}^{-1})$ configuration. The combined evidence from inelastic proton scattering and the present experiment identifies all 19 levels unambiguously. A simple shell model calculation that includes configuration mixing indirectly by using experimental matrix elements from two-particle states reproduces the energies very well. It also gives branching ratios, which are very sensitive to structural details, that agree with the experimental data quite well. Exceptional agreement is achieved for the $\frac{1}{2}^+$ and $\frac{3}{2}^+$ levels. In this case the wave functions could be determined from the measured branching ratios in a second independent way. The overlap with the wave functions calculated from the Hamiltonian is >97%. Still, there are many points that require better theoretical understanding, as, e.g., the transitions to the single-particle states.

The high-spin states above ~3.5 MeV show appreciable configuration mixing. Three levels of spin $\frac{19}{2}^+$ occur close to 3.5 MeV, whereas only one is expected below 3.6 MeV. This is yet to be understood.

The structure of 14 more levels for which approximate spins have been determined is completely open.

ACKNOWLEDGMENTS

The cooperation of the staff of the LANL Van de Graaff accelerator facility helped to make this work possible. Mr. Louis Maynard of LLNL contributed extensively to the experimental phase of this work. This work was performed under the auspices of the U.S. Department of Energy by the Lawrence Livermore National Laboratory under contract No. W-7405-ENG-48, and under contract No. PHY79-08395 between the National Science Foundation and the Florida State University. It was also supported by the Deutsches Bundesministerium für Forschung und Technologie.

---

*Present address: A. W. Wright Nuclear Structure Laboratory, Yale University, New Haven, CT 06511.

[1]T. P. Cleary, N. Stein, and P. R. Maurenzig, Nucl. Phys. A232, 287 (1974).

[2]W. T. Wagner, G. M. Crawley, and G. R. Hammerstein, Phys. Rev. C 11, 486 (1975).

[3]J. R. Beene, O. Häusser, T. K. Alexander, and A. B. McDonald, Phys. Rev. C 17, 1359 (1978).

[4]T. P. Cleary, N. Stein, W. D. Callender, D. A. Bromley, J. P. Coffin, and A. Gallman, Nucl. Phys. A232, 311 (1974).

[5]T. P. Cleary, W. D. Callender, and R. K. Sheline, Phys. Rev. C 21, 2244 (1980).

[6]P. D. Barnes, E. Romberg, C. Ellegaard, R. F. Casten, O. Hansen, T. J. Mulligan, R. A. Broglia, and R. Liotta, Nucl. Phys. A195, 146 (1972).

[7]J. W. Hertel, D. G. Fleming, J. P. Schiffer, and H. E. Gove, Phys. Rev. Lett. 23, 488 (1969).

[8]R. A. Broglia, J. S. Lilley, R. Perazzo, and W. R. Phillips, Phys. Rev. C 1, 1508 (1970).

[9]O. Häusser, F. C. Khanna, and D. Ward, Nucl. Phys. A194, 113 (1972).

[10]M. J. Martin, Nucl. Data Sheets 22, 545 (1977).

[11]C. Ellegaard, R. Julin, J. Kantele, M. Luontama, and T. Poikolaien, Nucl. Phys. A302, 125 (1978).

[12]T. Yamazaki, Nucl. Data A3, 1 (1967).

[13]M. B. Lewis, C. D. Goodman, and D. C. Hensley, Phys. Rev. C 3, 2027 (1971); 4, 284(E) (1971).

[14]J. Ungrin, R. M. Diamond, P. O. Tjom, and B. Elbek, K. Dan. Vidensk. Selsk., Mat.-Fys. Medd. 38, No. 8 (1971).

[15]A. Bohr and B. R. Mottelson, *Nuclear Structure* (Benjamin, New York, 1975), Vol. 2, p. 570ff.

[16]I. Hamamoto, Nucl. Phys. A126, 545 (1969); A135, 576 (1969); A148, 465 (1970).

[17]D. Zawischa, Z. Phys. 266, 117 (1974).

[18]K. Arita and H. Horie, Nucl. Phys. A173, 97 (1971).

[19]P. F. Bortignon, R. A. Broglia, D. R. Bes, and R. Liotta, Phys. Rep. 30C, 305 (1977).

[20]P. F. Bortignon, R. A. Broglia, D. R. Bes, R. Liotta, and V. Paar, Phys. Lett. 64B, 24 (1976).

[21]V. A. Khodel, A. P. Platonov, and E. E. Saperstein, J. Phys. G 6, 1199 (1980).

[22]S. Iwasaki, P. Ring, and P. Schuck, Nucl. Phys. A339, 365 (1980).

[23]*Table of Isotopes,* 7th ed., edited by C. M. Lederer and V. S. Shirley (Wiley, New York, 1978).

[24]C. V. K. Baba, T. Faestermann, D. B. Fossman, and D. Proetel, Phys. Rev. Lett. 29, 496 (1972).

[25]J. A. Becker, J. B. Carlson, R. G. Lanier, L. G. Mann, G. L. Struble, K. H. Maier, L. Ussery, W. Stöffl, T. Nail, R. K. Sheline, and J. A. Cizewski, Phys. Rev. C 26, 914 (1982).

[26]J. Blomqvist, private communication.